Carbohydrate Polymer Technologies and Applications 2 (2021) 100079

Contents lists available at ScienceDirect

Carbohydrate Polymer Technologies and Applications

journal homepage: www.elsevier.com/locate/carpta

Sustainable biomaterials based on cellulose, chitin and chitosan composites - A review

Marc Kostag, Omar A. El Seoud*

Institute of Chemistry, University of São Paulo, 748 Professor Lineu Prestes Av., São Paulo, SP 05508-000, Brazil

ARTICLE INFO

Keywords:
Fibers
Films
Hydrogels
Particles
Ionic liquids
Polysaccharide composites

ABSTRACT

In this review we describe recent advances of biocomposites consisting of cellulose, chitin, and chitosan. These polysaccharides are very important because they are abundant and renewable resources. As such, they significantly contribute to the development of sustainable processing of bioactive and biodegradable materials since there is an increased concern about the sustainability of synthetic polymers, leading to increased presence of microplastics in the environment. First, we briefly describe the molecular structures of cellulose, chitin, and chitosan. Our objective is to show that their related structural features lead to biopolymer dissolution in common solvents such as ionic liquids. We also address the dissolution mechanisms, biopolymer-solvent interactions, and solvent properties required to dissolve these biopolymers. Mutual solvents for of cellulose, chitin, and chitosan allow composite preparation via solution mixing which is advantageous with regard to processing complexity and costs. Thus, we present preparation, properties and application of cellulose/chitin/chitosan biocomposites in various physical forms, such as (nano)fibers, films, membranes, and hydrogels.

Abbreviations

AGU	Anhydroglucose unit
CA	Cellulose acetate
Cel/Ch/Chs	Cellulose/chitin/chitosan composite
CMC	Carboxymethyl cellulose
CNF	Cellulose nanofiber
DMF	*N,N*-Dimethylformamide
DMSO	Dimethyl sulfoxide
DA	Average degree of deacetylation of chitin
DS	Average degree of substitution of a cellulose derivative (maximum DS is 3)
I_c	Index of crystallinity
IL	Ionic liquid
H-bonds	Hydrogen bonds
MCC	Microcrystalline cellulose
MS	Molecular solvent
NC	Nanocomposite
NP	Nanoparticle
$ScCO_2$	Supercritical CO_2
SEM	Scanning electron microscopy
tex	tex describes the mechanical properties of filaments or fibers in the textile industry. It is a unit of linear mass density of fibers. It is defined as the mass in grams per 1000 m. They are often given in the unit of cN/tex (centi-Newton per tex)

1. Introduction

Polysaccharides such as cellulose, chitin and its partially diacetylated derivative chitosan are abundant and low-cost natural polymers (Bassas-Galia, Follonier, Pusnik, & Zinn, 2017; Dumitriu, 2004; John & Thomas, 2012; Klemm, Schmauder & Heinze, 2005; M. G. Peter, 2005a). They are nontoxic, biodegradable, and carry functional groups (-NH_2, -OH) that lead to their superior bio- and cytocompatibility (Vieira et al., 2011). Cellulose and chitin are two important and structurally related polysaccharides that provide structural integrity and protection to plants, and some animals, respectively (Gooday, Jeuniaux & Muzzarelli, 1986). Although synthetic polymers have the advantages of low cost and composition consistency, their applications are often limited by their poor biocompatibility and the potential toxicity of their degradation products. Additionally, there is an increased concern about the green aspects of the life-cycle of synthetic polymers, including sustainability of their production, and their disposal. E.g., the microplastics problem is just one aspect of the undesirable persistence of synthetic polymers in the environment (Brahney et al., 2020; Evangeliou et al., 2020; Shamshina et al., 2018). The current SARS-CoV2 pandemic highlighted this problem because of the concomitant increase in the use of, e.g., fossil fuel based personal protective equipment (Vanapalli et al., 2021).

Blending of different polymers is a technological approach to generate new composites with tailor-made properties (Kulshreshtha &

* Corresponding author.
E-mail address: elseoud.usp@gmail.com (O.A. El Seoud).

https://doi.org/10.1016/j.carpta.2021.100079
Received 23 December 2020; Received in revised form 15 April 2021; Accepted 16 April 2021

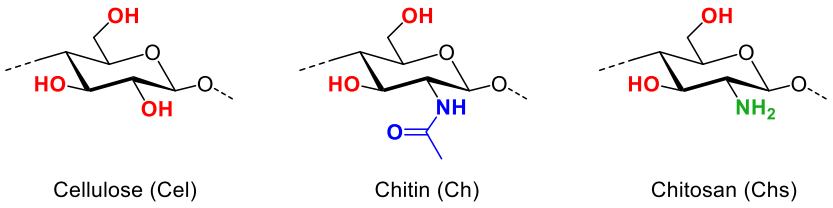

Fig. 1. Schematic representation of the repeating units of cellulose, chitin and chitosan. The number of CH_3–CONH-, NH_2-groups of chitin and chitosan depends on the average degree of deacetylation.

Vasile, 2002; Utracki, 1999), e.g., improved processability for the production of new fibers and materials for tissue engineering with properties superior to those of their precursor polymers. For example, the industrial application of pure chitosan is limited due to its weak mechanical strength, a problem that can be solved by using cellulose as reinforcement. Therefore, generating multifunctional, biodegradable composites by blending of biopolymers is an active field with emphasis on fabricating a broad range of materials for diverse applications, e.g., as films, foams, fibers, filters and nanoparticles, in addition to biomedical research in vitro, and potential applications in vivo (Díez-Pascual, 2019; Ebnesajjad, 2012; Kestur, 2010). E.g., tissue engineering, is the fastest growing segment in biomedical applications (Shamshina, Berton & Rogers, 2019); cellulose and cellulose acetate are being increasingly employed in ultra- and nanofiltration in the beverage and food industries (Galanakis, 2015); new opportunities for the use of biopolymers arise due to demands of the current pandemic (Galanakis, 2021).

In this review we cover literature of the last 5 years, *where applicable*, on Cel/Ch and Cel/Chs biocomposites mainly prepared by solution blending, i.e., dissolution of both biopolymers, separately or simultaneously, in compatible solvents (Takegawa, Murakami, Kaneko & Kadokawa, 2010), followed by processing into the desired "shapes". Solution blending is advantageous because it allows the preparation of biocomposites using, e.g., one-pot protocols which significantly reduce processing complexity and costs (Shamshina et al., 2018). The heterogeneous preparation of Cel/Ch and Cel/Chs composites by reinforcing chitin and chitosan matrices with cellulose nanofibers, cellulose nanocrystals, and bacterial cellulose or vice versa were reviewed recently and will not be considered herein (Khalil et al., 2016; Liu et al., 2020; Riva et al., 2015).

Before addressing the basis for the dissolution of cellulose, chitin and chitosan in common solvents, we first briefly discuss the molecular structures of these biopolymers with emphasis on the dissolution mechanisms, biopolymer-solvent interactions, and solvent physicochemical properties required for their dissolution. Subsequently, we discuss the preparation, properties and application of Cel/Ch/Chs biocomposites, with emphasis on fibers and nanofibers, films and membranes, as well as miscellaneous "shapes".

2. Common ground for the physical dissolution of cellulose, chitin and chitosan

2.1. Introduction to the molecular structures of cellulose, chitin and chitosan

Polymers in general are expected to mutually interact strongly if they carry specific groups that form efficient hydrogen bonds (H-bonds) in addition to non-specific interactions, e.g., van der Waals forces. As shown in Fig. 1, the repeating units of cellulose, chitin and chitosan are structurally related, and carry functional groups (CH_3–CONH-, NH_2, and OH) that are expected to interact strongly, hence form relatively homogeneous nanocomposites (NCs), as has been demonstrated experimentally.

The fabrication of NCs becomes simple if the component polymers dissolve in common solvents, because the desired product can be obtained by solution mixing, followed by casting and solvent removal. The composition of the NC, as well as some of its important physicochemical properties, e.g., mechanical and thermal, can be controlled by adjusting the concentrations of the precursor components. Therefore, we start by a brief discussion of the molecular structures of the above-mentioned biopolymers. Our goal is *to show their common structural features* that are expected to enhance their mutual interactions at the molecular level. This structural similarity is expected to lead to biopolymer dissolution in common solvents, as was shown, e.g., in case of ionic liquids (ILs). With this proviso(similar molecular structures interact strongly) it is expected that cellulose should form relatively homogeneous NCs with chitin and chitosan with good physicochemical properties, hence applications, as shown in Section 3.

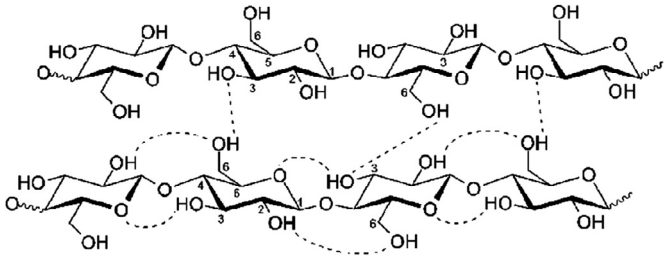

Fig. 2. Schematic representation of the intra- and intermolecular hydrogen bonding in cellulose; adapted with permission from Pinkert et al., (2010), ACS, 2010.

2.2. A brief description of the molecular structure of cellulose, chitin and chitosan

2.2.1. Cellulose

The cellulose molecule consists of (1→4)-linked β-D-glucose units, commonly referred to as anhydroglucose unit (AGU) (Heinze, El Seoud & Koschella, 2018; Pérez & Samain, 2010). The β-linkage results in twisting of each second AGU along the chain axis by 180° As argued elsewhere, the repeating unit of cellulose is the AGU, as shown schematically in Figure SI-1 (Fig. 1 of Supplementary Information) (French, 2017). The presence of three hydroxyl groups in each AGU leads to strong *intramolecular and intermolecular* H-bonds, as shown schematically in Fig. 2 (Gardner & Blackwell, 1974; Pinkert, Marsh & Pang, 2010). The formation of these H-bonds is responsible for the semi-crystalline structure of cellulose, with crystalline and amorphous domains.

Cellulose has an amphiphilic character because the equatorial direction of the glucopyranose ring has a hydrophilic character, whereas the axial direction of the ring is hydrophobic, see Figure SI-2. The relative importance of hydrophobic/solvophobic interactions for cellulose properties, in particular its lack of dissolution in water and dipolar aprotic solvents was recently discussed in details. In summary, the cellulose molecules are linked together in a layer by stacking of glucopyranose rings; the layers are held together by non-specific interactions and weak C–H•••O bonds (Glasser et al., 2012; Medronho & Lindman, 2015). Our recent data on cellulose dissolution in mixtures of dimethyl sulfoxide (DMSO) with ILs showed that both factors, H-bonding and solvophobic interactions have comparable relevance to cellulose dissolution (O. A. El Seoud, Bioni & Dignani, 2020).

Central to the structural features of cellulose is its crystallinity. Thus, the biopolymer exists in several allomorphic forms; cellulose I_α and cel-

lulose I_β are the predominant ones (Hayashi, Sugiyama, Okano & Ishihara, 1997). Several cellulose allomorphs are obtained through different treatments, in particular the thermodynamically more stable cellulose II is obtained by mercerization. Consequently, one of the fundamental properties of any cellulose sample is its index of crystallinity (I_c), most frequently calculated from X-ray diffraction data (Buschle-Diller & Zeronian, 1992; Driemeier & Calligaris, 2011; Segal, Creely, Martin, J. & Conrad, 1959). Other techniques for probing cellulose allomorphs, and for the calculation of I_c include 1D and 2D ^{13}C NMR cross-polarization magic angle spinning (Foston, 2014; (Wang et al., 2016b)); FTIR and NIR spectroscopy (Xu et al., 2013b). Typical values of I_c of cellulose samples are 0.6 ± 0.1 (Poletto, Ornaghi & Zattera, 2014).

The above-discussed structural features of cellulose have several important consequences on its processing. Unlike many synthetic polymers, cellulose cannot be processed by injection molding, or extrusion from the melt. The reason is that its melting temperature presumably lies above its temperature of thermal decomposition. Another aspect is that many protic solvents (water and alcohols) and strongly dipolar aprotic solvents only cause swelling, but do not dissolve cellulose (Boluk, 2005; Fidale, Ruiz, Heinze & El Seoud, 2008; Philipp, Schleicher & Wagenknecht, 1973). Thus, a strong dipolar character of the solvent is a required, but not sufficient property for cellulose dissolution, see below, section 2.3.

2.2.2. Chitin

Chitin ((1→4)−2-acetamido-2-deoxy-β-D-glucan) the second most abundant biopolymer in nature, after cellulose (Gooday, 1990). It is the building material that gives strength to the exoskeletons of crustaceans (M. G. Peter, 2005a), and the cell walls of fungi (M. G. Peter, 2005b). The term chitin is derived from the Greek word “chiton”, meaning a coat of mail (i.e., a garment of metal scales or chain mail worn as armor) (El-Diasty, Nesreen & Hoda, 2012). Crab, krill, lobster and shrimp are the main commercial sources of chitin (Johnson & Peniston, 1982), with approximate chitin contents (on dry bases) of 26, 24, 60 to 75, and 18 wt%, respectively (Hamed, Özogul & Regenstein, 2016). Estimates of global annual production of some crustaceans are: Crab, 405.400 tons in 2018; Lobster, 150.000 tons in 2017 (Food & Agriculture Organization of the United Nations, 2019); and Shrimp, 4.8 million tons in 2019 (Anderson, Valderama & Jory, 2019), leading to more than one million tons of raw material for processing into chitin.

Crustacean chitin is closely associated with proteins, lipids, minerals, and pigments. The industrial chitin extraction process involves three basic steps: (i) deproteinization for removal of the proteins, e.g., with aqueous solutions of sodium- hydroxide, carbonate, hydrogen carbonate, sulfide, sulfite, hydrogen sulfite, and trisodium phosphate; potassium- hydroxide and carbonate, and calcium hydroxide (Lodhi et al., 2014); (ii) demineralization with acid for removal of calcium carbonate, e.g., with aqueous solutions of HCl, and other acids, e.g., nitric, sulfuric, acetic, and formic; HCl is most the employed (No & Hur, 1998; Percot, Viton & Domard, 2003; Younes & Rinaudo, 2015); and (iii) decolorization for removal of pigments, e.g., by extraction with ethanol, acetone, or bleaching with hydrogen peroxide (Laurienzo, 2010). The first two steps can also be performed by a biological route with less environmental impact using, e.g., proteases-producing bacteria, followed by treatment with lactic acid (Khanafari, Marandi & Sanatei, 2008). Scheme SI-1 shows these steps, as well as the conversion (chitin → chitosan) that will be discussed below.

As in the case of cellulose, the individual *N*-acetylglucose units in chitin are rotated 180° with respect to each other, so that every two units form the disaccharide *N,N´*-diacteylchitobiose (Muzzarelli, 2013). Because enzymatic hydrolysis of chitin leads to the production of *N*-acetylglucosamine and glucosamine, it was presumed that latter is present as a significant fraction of the polymer. However, solid-state NMR analysis of chitin suggested that little, or no glucosamine is present (Kramer, Hopkins & Schaefer, 1995). Chitin tends to form microfibrils (also referred to as rods or crystallites) of ca. 3 nm in diameter that are stabilized by H-bonds, involving the *N*-glucoacetate residue and hydroxyl groups. Chitin microfibrils of peritrophic matrices may even exceed 0.5 μm in length and are frequently associated in bundles containing parallel groups of 10 or more single microfibrils (Lehane, 1997).

X-ray diffraction analysis suggested that chitin is a polymorphic substance that occurs, as in the case of cellulose, in three different crystalline modifications termed α-, β-, and γ-chitin (Blackwell, 1988). They mainly differ in the degree of hydration, in the size of the unit cell, and in the number of chitin chains per unit cell (Kramer & Koga, 1986). As Figure SI-3 shows, all chains exhibit antiparallel orientation in the α-form, whereas they are arranged parallel in the β-form. In γ-chitin, the biopolymer forms set of two parallel strands alternative with a single antiparallel strand, i.e., two chains “up” for each one “down”. Additionally, non-crystalline, transient states have also been reported in a fungal chitin (Vermeulen & Wessels, 1986).

The chitin molecules were found to be packed tightly by relatively strong H-bonds between -C2-C $\underline{O}$–$NHCH_3$ of the *N*-glucoacetate residue, and -C2CO–N $\underline{H}CH_3$ of an adjacent *N*-glucoacetate residue, and with C3-$\underline{OH}$ and $C6CH_2-$ $\underline{OH}$ groups. Fig. 3 shows the X-ray based crystalline structures of α- and β-chitin. In the crystalline structure of the former polymorph (most abundant in nature), the unit cell is orthorhombic with $a = 0.47$, $b = 1.886$, and c (fiber axis) = 1.032 nm with a space group of $P2_12_12_1$. The cell contains chitobiose sections of two chains passing through the center and corner of the (ab) projection of the unit cell where each chitin chain takes helical conformation (zigzag structure). The direction of the center and corner chains of the unit cell is opposite along the c-axis (Gardner & Blackwell, 1974, 1975). The unit cell of β-chitin is monoclinic with $a = 0.845$, $b = 0.926$, and c (fiber axis) = 1.038, and $\gamma = 97.5°$. The conformation of the β-chitin chain is an extended twofold helix similar to that of α-chitin, except that the β-chitin molecules are packed in a parallel fashion, and the unit cell is packed with only one chitin chain. Unlike α-chitin, the chains of the β-chitin polymorph form H-bonded sheets along the a-axis, with no inter-sheet H-bonding along the b-axis. This difference explains the fact that β-chitin (e.g., from squid pens) exhibits more swelling by protic and aprotic solvents, and is more reactive toward derivatization than α-chitin (e.g., from crab, lobster, krill and shrimp) (Pillai, Paul & Sharma, 2009; Tokura & Tamura, 2007; Younes & Rinaudo, 2015).

2.2.3. Chitosan

Chitosan is usually obtained by chemical or enzymatic deacetylation of chitin, concomitant depolymerization of the precursor biopolymer may occur as well. The distinction between chitin and chitosan can be made on the bases of degree of deacetylation (DA). When the DA is higher than 50 mol%, the product is designated as chitosan, and is soluble in dilute acid solutions (Roberts, 1992). Heterogeneous *N*-deacetylation is carried out by suspending chitin in hot, concentrated alkali for several hours (Chang, Tsai, Lee & Fu, 1997). Homogeneous deacetylation is performed by suspension of chitin in a concentrated base; biopolymer dissolution is obtained by quick cooling below 5 °C using crushed ice. Compared to the heterogeneous deacetylation, the DA is lower. At DA of 48% – 55% the product is soluble and the acetyl groups are uniformly distributed along the chains (Kurita, Sannan & Iwakura, 1977; Sannan, Kurita & Iwakura, 1976). Alternatively, chitin dissolution and homogeneous deacetylation was carried out in ionic liquids (ILs), e.g., tetraalkylammonium hydroxides (Q. Ma et al., 2020; Shimo, Abe & Ohno, 2016). The environmentally friendly enzymatic route for the chitin → chitosan conversion uses chitin deacetylases. It is a controlled, non-degrading process, resulting in the production well-defined chitosan structures by catalyzing the hydrolysis of *N*-acetamido bonds in chitin (Araki & Ito, 1974; Martinou, Kafetzopoulos & Bouriotis, 1993; Tsigos, Martinou, Kafetzopoulos & Bouriotis, 2000).

In the solid state, chitosan is a semicrystalline polymer. The X-ray based crystal structures of hydrated chitosan is shown in Figure SI-4. Each chitosan chain takes an extended two-fold helix, i.e., a zigzag structure. As in case of chitin, chitosan chains on c-axis are the “up chains”

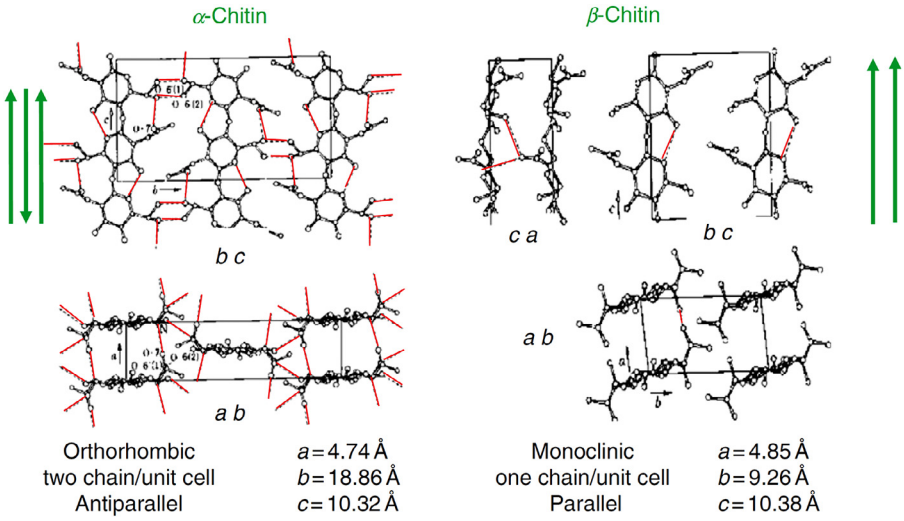

Fig. 3. X-ray-based representation of the H-bonds present in α-chitin (left) and β-chitin (right); adapted with permission from Gardner and Blackwell, (1975), Wiley, 1975; and (Tokura & Tamura, 2007), Elsevier, 2007.

whereas, those in the unit cell are "down chains". That is, chitosan chains are packed in an antiparallel fashion. Along the b-axis, the up- and down-chains are H-bonded, leading to stacked sheets along the a-axis. The sheets are H-bonded by the intercalated water molecules (Figure SI-4 b). This polymorph is the most abundant in chitosan samples. Heating the chitosan sample (annealing) results in a somewhat similar structure, the chains are packed in an antiparallel mode. Because of the absence of water, the chains are directly H-bonded (Ogawa, Yui & Okuyama, 2004).

2.3. Common solvents for the physical dissolution of cellulose and chitin/chitosan

Here we address biopolymer *physical* dissolution, i.e., without covalent bond formation. As shown above, the discussion on common solvents for cellulose, chitin and chitosan is relevant to the fabrication of their NCs using the simple strategy of mixing of biopolymer solutions, followed by NC regeneration in different physical forms, e.g., films or nanoparticles, NPs. As we indicated, the molecular and crystalline structures of the three biopolymers are related. It is expected, therefore, that the interactions of the solute (the biopolymer) with the solvent are similar. In aqueous solutions of chitin and chitosan, hydrophobic interactions depend on the degree of deacetylation because of the hydrophobic nature of the acetamido residues (Philippova et al., 2012). Note that chitosan is soluble in dilute acid solutions due to protonation of its free NH_2 groups, whereas cellulose is soluble in concentrated acids, e.g., formic and trifluoroacetic acids due to formation of the corresponding esters, cellulose formate and trifluoroacetate, respectively (Hasegawa, Isogai, Onabe & Usuda, 1992; Köhler, Liebert & Heinze, 2009).

Based on the above-shown structural similarities, it can be safely stated that the requirement for the physical dissolution of the three biopolymers is solvent-induced disruption of specific (H-bonding) and non-specific (e.g., van der Waals, hydrophobic) interactions present (Morais et al., 2020; Philippova et al., 2012; Taheri, Abdolmaleki & Fashandi, 2018). Because much more work was done on the dissolution of cellulose, we concentrate on this biopolymer, and give the corresponding data for chitin and chitosan, where available (Shamshina, 2019) . We limit our discussion to ionic solvents, e.g., pure ILs, and *solvent systems* composed of two or more components, in particular aqueous LiOH or NaOH/urea (J. Cai & Zhang, 2005; Luo & Zhang, 2013; Zhou & Zhang, 2000) and solutions of ILs in water and in molecular solvents (MS). Deep eutectic solvents, e.g., those composed of choline chloride and urea will not be discussed because of their (until present) limited capacity to dissolve cellulose hence applications (Chen, Zhang, You & Xu, 2019; Tenhunen et al., 2018).

At the outset, we show a simplified mechanism for the dissolution of cellulose, chitin and chitosan. In principle, this mechanism applies to the dissolution in pure ILs. However, we discuss the more "practical" approach of using IL/MS binary mixtures because their use leads to lower biopolymer solution viscosity, hence better mass and heat transfer. Note that in many cases, IL/MS mixtures dissolve more biopolymer than pure IL, due to enhanced ionization of the IL (O. A. El Seoud, Kostag, Jedvert & Malek, 2020; Kostag, Gericke, Heinze & El Seoud, 2019; A. Xu et al., 2013). For simplicity, the biopolymer-IL/MS interactions are depicted as occurring in a stepwise manner although they are, most certainly, cooperative. This cooperativity is indicated by theoretical calculations and FTIR data on H-bonding in 1-butyl-3-methylimizaloium salts (chloride, bromide, and tetrafluoroborate) (Liu, Kim, Dhumal & Kim, 2019), and interactions of glucose oligomers with 1-ethyl-3-methylimidazolium acetate (Ishida, 2020). Thus, the anions of the IL form H-bonds with the hydroxyl groups of the same AGU, or the aminoglucose residues, as well as adjacent monomers, as shown by molecular dynamics simulations (Ishida, 2020; Parviainen et al., 2013; Pires et al., 2015). The negatively charged anion-biopolymer complexes start to separate due to electrostatic repulsion. This separation is enhanced by "condensation" of the (usually voluminous and asymmetric) cations in order to maintain electric charge neutrality. The steric repulsion between the chains of the biopolymer-IL/MS complex causes concomitant disruption of the non-specific interactions, and eventually leads to biopolymer dissolution, as illustrated in Fig. 4 (O. A. El Seoud et al., 2020; A. Xu et al., 2013).

Regarding H-bonding, the solvent acts either as an acceptor of the electron lone-pair from the hydroxyl group, i.e., Cel- $\underline{O}$(H)•••HS (S = solvent, acting as a Lewis acid) or as electron-pair donor Cel-O- $\underline{H}$••••SH (S is acting as a Lewis base), or both. Consequently, we start by showing how these properties (or solvent descriptors) are *quantified* using solvatochromism. The latter term refers to the effect of the solvent, pure or mixture, on the spectra, absorption or emission, of certain substances (solvatochromic probes, or simply probes) whose spectra are sensitive to the physiochemical properties of the solvent, due to probe-solvent interactions. The latter interactions are clearly manifested as shifts of the values of the probe λ_{max}, e.g., relative to that in a reference solvent, e.g., tetramethylsilane (Reichardt & Welton, 2010). Some representative probes are shown in Figure SI-5, along with the solvent descriptors that are calculated by manipulation of their spectral data. These descriptors include the empirical, or total solvent polarity, E_T(probe), solvent Lewis acidity (*SA*) and Lewis basicity (*SB*), its dipolarity (*SD*), and polarizability (*SP*). In a recent study on solvatochromism, and cellulose dissolution

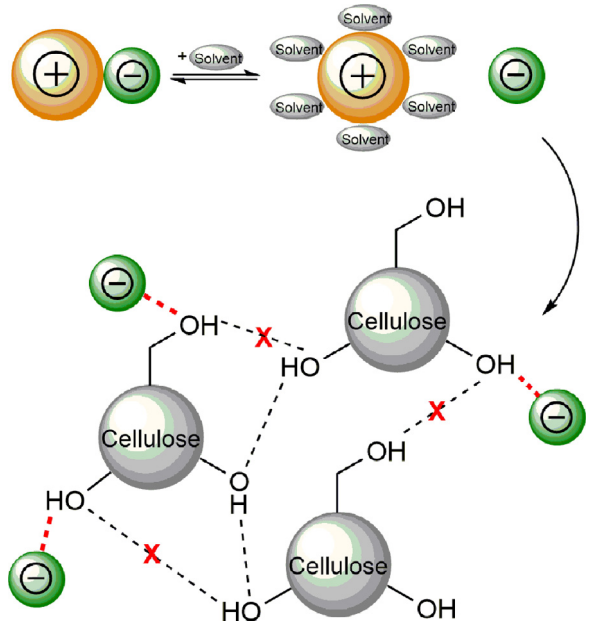

Fig. 4. A simplified scheme for cellulose dissolution by a typical IL, anions of the latter form H-bonds with the hydroxyl groups of the AGU; "condensation" of the large, asymmetric cations leads to cellulose chain separation and biopolymer dissolution; reproduced with permission from O. A. El Seoud et al., (2020), Wiley, 2020.

by mixtures of IL/DMSO (O. A. El Seoud et al., 2020), we showed that substitution of SD by the molar volume of the IL, V_M, and *SP* by the Lorentz-Lorenz function of the refractive index of IL/DMSO, *f(n)* gives better correlations.

A brief description of the use of solvatochromism for assessing solvent efficiency is in order. We start by showing the correlation between these solvent descriptors:

$$E_T(probe) = E_T(probe)_0 + aSA + bSB + dSD + pSP \quad (1)$$

$$E_T(probe) = E_T(probe)_0 + aSA + bSB + dV_M + pf(n) \quad (2)$$

That is, the solvent empirical polarity term includes all probe-solvent specific interactions and their non-specific counterparts. Except for V_M and *f(n)*, all other solvent descriptors are calculated by manipulation of the spectral data of the probes. For example, E_T(probe) is calculated from Eq. (3), where λ_{max} is the maximum wavelength of the solvatochromic (i.e., solvent sensitive) peak (Reichardt & Welton, 2010), where the probe WB is that shown in Figure SI-5.

$$E_T(WB),\ kcal/mol = 28591.5/l_{max},\ nm \quad (3)$$

To calculate specific properties, for example *SA*, a pair of homomorphic probes (e.g., TBSB and DTBSB; Figure SI-5) is usually employed. The first, TBSB, is related to Lewis acidity of the solvent, in addition to non-specific probe-solvent interactions. Because of steric crowding around the phenolate oxygen that suppresses probe••••• HS H-bonding, the second probe, DTBSB, is sensitive only to non-specific interactions (Catalán & Díaz, 1997). The value of *SA* is then calculated by manipulating the spectral data of this pair of probes. *SB* is calculated similarly by manipulating the UV/Vis spectral data of NI (related to Lewis basicity of the solvent and non-specific probe-solvent interactions) and MNI (related to non-specific interactions) (Catalán, 2009).

Therefore, solvent efficiency can be *predicted* from the values of the solvent solvatochromic parameters. An example of this prediction is that ILs with effective basicity (= *SB* − *SA*) in the range 0.35 < *SB-SA* < 0.9 are expected to be good cellulose solvents (Hauru, Hummel, King, Kilpeläinen & Sixta, 2012; Parviainen et al., 2013). A similar conclusion was reached regarding the importance of *SB* to the dissolution of chitin (SB > 0.5), independent of the value of *SA*. In fact, the chitin dissolution capacity of (protic) IL tris(2-hydroxyethyl)methylammonium hydroxide was enhanced by adding ethylenediamine to the medium. Addition of the latter base decreased *SA* and increased *SB,* i.e., increased the solvent effective basicity (Shimo et al., 2016). The importance of *SB* for the dissolution of chitin was also corroborated by molecular dynamics simulations (Uto, Idenoue, Yamamoto & Kadokawa, 2018).

Our recent study on cellulose dissolution IL/DMSO mixtures quantified, *for the first time*, the relative importance of the solvent descriptors shown in Eq. (2), and *highlighted* the requirements for efficient solvents for this biopolymer. Eq. (4) and Eq. (5) show the dependence of the mol fraction of dissolved MCC (MCC-χ) at 70 °C, on solvent descriptors for 11 IL/DMSO mixtures, based on substituted imidazoles and 1,8-Diazabicyclo(5.4.0)undec-7-ene, and for 9 IL/DMSO mixtures based only on substituted imidazoles. As shown by the regression coefficients of these equations, MCC/solvent H-bonds (the *SA* and *SB* terms), and non-specific interactions (the *f(n)* term) are important and favor cellulose dissolution; *SB* is more relevant than *SA*. On the other hand, the solvent efficiency decreases as a function of increasing its molar volume (the V_M term) and the solvent structure rigidity, as discussed elsewhere (Hanabusa et al., 2018). Thus, some ILs that carry (rigid) phenyl groups are not efficient cellulose solvents, e.g., tribenzylmethylammonium acetate because of steric hindrance to solvent penetration into the biopolymer structure (Kostag & El Seoud, 2019).

The advantage of using the mol fraction scale to report cellulose dissolution is that it permits calculation of the *average* number of solvent species (IL and DMSO) required to dissolve each AGU under the experimental conditions. These numbers are (IL name, number of IL, and DMSO molecules required to dissolve each AGU, respectively): 1-ally-3-methylimidazolium acetate, 3.4, 2.3; 1-allyl-2,3-dimethylimidazolium acetate 3.9, 2.6; 1,8-diazabicyclo[5.4.0]undec-7-ene-8-ium acetate 7.3, 5.2, and tetramethylguanidinium acetate 11.1, 7.4. The efficiency of the imidazole-based ILs as cellulose solvents is clear (O. A. El Seoud et al., 2020).

$$MCC - c = 74.32 + 23.70SA + 52.74SB - 22.02V_M + 30.02f(n) \quad (4)$$
$$(11\ L/DMSO, R^2 = 0.872)$$

$$MCC - c = 119.84 + 3.64SA + 15.50SB - 68.6V_M + 46.04f(n) \quad (5)$$
$$(9IL/DMSO; R^2 = 991)$$

3. Preparation, properties and selected applications of cellulose/chitin/chitosan biocomposites

The literature presented below discusses some biomedical applications of Cel/Ch/Chs composites. This is not surprising because one of the components (chitin, chitosan) possesses biological activity; both components are biodegradable. As example, antimicrobial activity against many bacteria and fungi is most likely mediated by electrostatic interactions between positively charged amino groups of chitin and chitosan (pK_a of chitosan = 6.5) and the negatively charged microbial cell membrane (Deng, Wang, Chen & Liu, 2020). Chemical modification of the biopolymers often increases solubility and even enhances biological interactions (Martínez-Campos et al., 2017), as can be deducted from the discussion below. On the other hand, chitin and chitosan microbial activity may be reduced by suppressing amino group protonation, e.g., by introducing substituents (G. Ma et al., 2008). Note that while chitosan protonation increases dramatically its swelling ratio in water (ca. 1500%) due to the Gibbs–Donnan effect, and solubility, it may also lead to significant weight loss (leaching) when the composite possesses high chitosan content. The protonation of cellulose is not an issue under the usual application pH range employed (3 to 8), because of its high pK_a (J. Yang, Dahlström, Edlund, Lindman & Norgren, 2019). *In principle*, the same discussion applies to anionic or cationic modified chitin/chitosan and cellulose derivatives.

3.1. Fibers and nanofibers

The primarily important characteristics of Cel/Ch/Chs composite fibers are their mechanical and biological properties. Mechanical strength is needed when the fibers are subjected to higher mechanical stress such as in sutures, wound dressings, or coatings of flexible materials such as textiles. In case of Cel/Ch/Chs composite fibers, strength increases with increasing content of cellulose that represents the rigid component relative to chitin and chitosan. E.g., a Cel/Chs composite fiber with a weight ratio of 1:1 has a 3-fold higher strength compared to neat chitosan (Mikhailov, Lebedeva, Nud'ga & Petrova, 2001). Composite fibers for (implantable) medical applications should be biologically inert, namely, they should not cause, or promote complications or tissue reaction. Ideally, they should lose strength at the same rate that the tissue gains strength (n.a., 2020). Thus, the complementary properties of cellulose and chitin/chitosan are ideal for composite fiber fabrication.

A simple and sustainable one-pot process was reported on the fabrication of electrospun transparent nanomats. Chitin was extracted from shrimp shell, followed by co-dissolving MCC and chitin in 1-ethyl-3-methylimidazolium acetate (Shamshina et al., 2018). To obtain the spinning dope, 2 wt% ground and sieved shrimp shells were stirred in the IL with microwave heating. After centrifugation to remove the insoluble components, ~0.6 wt% chitin remained in the IL (see Scheme SI-1). The overall polymer concentration of chitin and cellulose was then adjusted to 0.4 wt% for optimal electro-spinnability. The fabricated electrospun nanomats (7:3 chitin/MCC) demonstrated a 2-fold improvement in hardness and 3-fold improvement in elasticity compared to pure chitin nanomats. Addition of more MCC resulted in worsening of these mechanical properties. Shifting the polysaccharide composition further towards MCC (1:1 by weight) led to non-spinnable dopes because the spun jet broke into droplets, regardless of solution flow. Therefore, a sufficiently high solution viscosity of polymer/IL solutions is a determining factor for spinnability (Zavgorodnya, Shamshina, Bonner & Rogers, 2017).

Blood-compatible, heparin-like composite fibrous membranes were fabricated through electrospinning of chitosan together with ethylcellulose in ethanolic solution onto bacterial cellulose sulfate. Chitosan NPs were obtained by ball milling of commercial chitosan powder; cellulose sulfate was synthesized by sulfation with SO_3/pyridine. Ethanolic solution of ethylcellulose and chitosan was electrospun on an aluminum foil covered with cellulose sulfate. SEM images revealed that there were no chitosan NPs on the surface of the spun material, indicating that chitosan had been stretched to nanofibers. Blood compatibility of the composite membrane was assessed with coagulation time, inflammatory response, and platelet adhesion experiments. The obtained membranes exhibited good blood compatibility, no platelets adhered on the surface; macrophages seeded on the membranes are not activated after 24 h incubation (Li et al., 2018).

Electrospun CA/chitosan nanofibers containing single walled carbon nanotubes, Fe_3O_4, and TiO_2 were investigated regarding their efficiency to remove of Cr(VI), As(V), methylene blue and Congo red dyes from aqueous solutions (ZabihiSahebi et al., 2019). The electrospinning solution was prepared by dissolving 7.2 wt% chitosan and 4.8 wt% CA in a trifluoroacetic/dichloromethane mixture (70:30 by volume) and dispersing single walled carbon nanotubes/Fe_3O_4/TiO_2 in the obtained solution. The electrospun nanofibers (Figure SI-6) were successfully reused for five adsorption/desorption cycles under optimum pH of 3. As mentioned above, chitosan leaching because of the employed acidic conditions may limit this application.

Aqueous solutions containing (by weight) LiOH/urea/H_2O (4.5: 15 : 80.5) and LiOH/KOH/urea/H_2O (4.5 : 7 : 8 : 80.5) were used as solvents for cellulose and chitosan, respectively (Zhu et al., 2019). The spinning solution was obtained by mixing cellulose and chitosan solutions, in a weight ratio of 1:1 with an overall polymer concentration of 5 wt%. The fibers were wet-spun into 15 wt% phytic acid aqueous solution at 5 °C. The tensile strength of the composite fiber (2.3 cN/dtex) was much higher than those reported for Cel/Chs composite fibers spun from ILs (1.86 cN/dtex) or the viscose fiber (1.8–2.5 cN/dtex; see Abbreviations and Acronyms for the definition of tex). The improved mechanical properties were attributed to the acidic coagulation conditions. The acid destroys the alkali/urea complex solvation layer and the exposed cellulose and chitosan chains align parallel to form nanofibers *via* strong self-aggregation force without fibrillation (Fig. 5).

Cellulose, chitosan, polyvinylamine and citric acid (used for the first time as crosslinking agent for these biopolymers) were used to produce a water-stable, low-density fiber foam (density 0.33–0.66 g cm^3) packaging material with antimicrobial properties (Ottenhall, Seppänen & Ek, 2018). The latter properties were assessed on *E. coli* and *Aspergillus brasiliensis*. To obtain the foam material, chitosan or polyvinylamine were dissolved in citric acid and the cellulose pulp was suspended in the resulting solution, followed by addition of sodium dodecyl sulfate as a foaming agent. The cellulose foams containing chitosan had both good water-stability and good antibacterial and antifungal properties, while the foams containing polyvinylamine disintegrated in water and did not inhibit fungal growth.

3.2. Films and membranes

A major application for (bio)plastic films and membranes are packaging materials, especially for the important field of functional food packaging (Ludwick & Aglan, 2020). This application includes processing, transporting, distributing, and retailing of food, and preserving it from external contamination (Haghighi, Licciardello, Fava, Siesler & Pulvirenti, 2020). In particular the latter appears to be of high interest during the current COVID-19 pandemic crisis in order to avoid the cross-contamination and spreading of the virus between the various stages of the supply chain (Galanakis, 2020). Furthermore, recent concern about material sustainability prompted the search for biodegradable and compostable materials based on renewable resources, in particular from cellulose, chitin and chitosan because of their abundance and favorable mechanical and biological properties (Kumar, Mukherjee & Dutta, 2020; Priyadarshi & Rhim, 2020; H. Wang, Qian & Ding, 2018).

Films fabricated from chitosan and carboxymethyl cellulose (CMC) are extensively studied because they build strong polyelectrolyte complexes (Fukuda, 1980). *Hu* et al. used CMC and the cationic 2-*N*-hydroxypropyl-3-trimethylammonium chloride derivative of chitosan to prepare composite films (Hu, Wang & Wang, 2016). Compared with the neat chitosan derivative film, the incorporation CMC improved tensile strength, thermal stability, and water resistance. With increasing CMC content, however, increased oxygen permeability, and decreased light transmittance and antibacterial activity was observed. It was concluded, that composite films containing 10–30 wt% CMC represent a good compromise for functional food packaging. By incorporating other additives, the composite properties can be modified. Thus, the effect of adding ZnO–NPs to Chs/CMC composites was studied and the physical, chemical and mechanical properties of the composites examined (Youssef, EL-Sayed, EL-Sayed, Salama & Dufresne, 2016). These authors mixed 1 wt% chitosan solution in dilute acetic acid with 1 wt% aqueous CMC solution at 1:1 vol ratios and added different concentrations of ZnO–NPs (2, 4, 8 wt%). Besides increased shelf life of white cheese, the composite films displayed good antibacterial activity against gram positive (*S. aureus*), gram negative (*P. aeruginosa, E. coli*) bacteria, and fungi. Comparable results were reported for Chs/Cel acetate-phthalate/ZnO composite films (Indumathi, Saral Sarojini & Rajarajeswari, 2019). Films loaded with 5 wt% ZnO NPs exhibited optimal mechanical properties combined with extended shelf life; they are biodegraded within 4 weeks.

By incorporating cinnamon essential oil and glutaraldehyde crossing agent, mechanical, physical, antimicrobial, and antioxidant properties of Chs/CMC/oil composite films were improved relative to their (cross-linked) Chs/CMC counterparts. The SEM images of these films (Figure SI-7) reveal dense, homogeneous, and smooth surfaces. Crosslinking and inclusion of cinnamon essential oil resulted in significantly

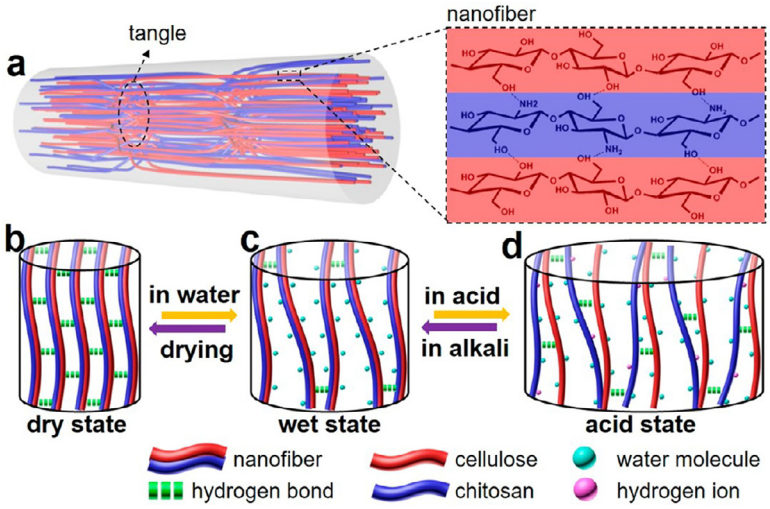

Fig. 5. (a) Structure of the Cel/Chs composite fiber and hydrogen bonding between both polysaccharides; (b) dry state of the fiber with hydrogen bonds formed between the polymer chains; (c) in the wet state water disrupts partly the hydrogen bonds between the nanofibers while the whole fiber stays intact (d) protonation of the chitosan component in acidic solution leads to separation of the nanofibers; reproduced with permission from Zhu et al., (2019), ACS, 2019.

higher mechanical strength, lower water vapor permeability, higher and steady state antioxidant activity, as well as in vitro antimicrobial properties against *Listeria monocytogenes* and *Pseudomonas aeruginosa*. Additionally, these films showed antioxidant activity (> 24 h) due to the presence of free NH_2 groups along the chitosan backbone, which reacts with free radicals (Valizadeh, Naseri, Babaei, Hosseini & Imani, 2019). All polysaccharide based composite films consisting of CMC, chitosan, sodium alginate, and $CaCl_2$ (cross-linking agent) were fabricated. The films were cast from aqueous solutions, dried at 60 °C, and stored at 25 °C at 50 % relative humidity. Chemometrics was employed to optimize the best film composition with regard to tensile strength, water vapor permeation rate, elongation at break, and antibacterial activity. The best film composition (in wt%; 1.5 : 0.5 : 1.5, CMC, chitosan, and sodium alginate, respectively) showed a tensile strength of 84.2 ± 12.9 MPa, and exhibited a smooth, uniform surface (SEM), indicating that the proportion and concentration used during the formation process facilitated even dispersion of CMC and chitosan within the polymer matrix, as well as good adhesion with the polymer matrix. The best composition film exhibited 95.7% ± 5.4% and 93.4% ± 4.7% against *E. coli* and *S. aureus* bacteria, respectively (Lan, He & Liu, 2018).

In another approach, cellulose and chitosan were simultaneously dissolved in 60 wt% aqueous LiBr (6.9 mol L^{-1} electrolyte) solution at 120 °C (J. Yang, Kwon, Hwang & Kim, 2018). Films with an increasing chitosan content with up to 30 wt% were slightly more robust (tensile strength, elongation, and E-modulus) and possessed greater antibacterial properties as tested against *E. coli* and *S. aureus*. It is likely that polymer degradation has occurred under these conditions.

Biodegradable composite films based on water soluble chitosan ascorbate (0.5 wt%) and methylcellulose (0.5 wt%) of different composition ratios (4:1, 2:1, 1:1, 1:2, 1:4 by volume) in the presence of glycerol plasticizer (0.15 wt%) were casted and compared to their pure polysaccharide derivative films (Tan et al., 2020). The tensile strength and elongation at break increased; water vapor permeability decreased as a function of increasing methylcellulose content. Higher chitosan ascorbate content led to better antioxidant properties and barrier properties against UV/vis. The chitosan ascorbate/methylcellulose composite films with interesting physicochemical properties and strong antioxidant action showed the potential value as biodegradable and edible biomaterials for food packaging.

Multilayer films were obtained through layer-by-layer assembly of CMC and chitosan on a surface modified Si wafer. First, the latter was coated with (3-glycidoxypropyl)trimethoxysilane layer, then it was immersed in a CMC solution (pH = 4; CMC = 1 mg/mL), rinsed with water, immersed in a chitosan solution (pH = 4; chitosan = 1 mg/mL), rinsed with water; the complete procedure was repeated 5 to 6 times. The deposited bilayers were also subjected to cross-linking by dipping the loaded Si wafer into an aqueous mixture of *N*-hydroxysulfosuccinimide and 1-ethyl-3-(3-(dimethylamino)propyl)-carbodiimide, followed by immersion in glutaraldehyde solution to complete the cross-linking; see Fig. 6. As shown from the results of SEM, atomic force microscopy, and gas adsorption, the cross-linking treatment increased the film thickness (7.1%), roughness (67.6%), and porosity (3150%). Both types of films were loaded with model drugs, whose release was followed by fluorescence measurement. Interestingly, more of the small-molecule drug model (fluorescein isothiocyanate) was loaded into and released from the non-cross-linked multilayer film, whereas more of the macromolecular drug model (ovalbumin) was loaded into and released from the cross-linked multilayer film. That is, drug loading/release can be controlled according to the molecular weight of the desired drug by changing the structure of the film (Park, Choi, Jeong, Heo & Hong, 2017).

Besides the antimicrobial properties of Cel/Ch/Chs composites, the mechanical properties are of fundamental importance and can be tailored to the desired application. They depend on the polymers molecular structure and composition. Therefore, we discuss selected examples of controlling the mechanical properties of composite films. A heterogeneous approach was employed by adding small amounts of cellulose filter paper to a solution of chitosan in acetic acid (Z. Wang et al., 2009). A weight ratio cellulose/chitosan of 1:100 improved the mechanical strength of the composite compared with pure chitosan. This was partially attributed to the formation of Schiff-base between the chitosan matrix and cellulose. The latter carries aldehyde groups formed during its (industrial) bleaching step. pH-Responsive Cel/Chs films of different compositions were prepared in aqueous solutions; the biopolymers were dissolved separately (J. Yang et al., 2019). Thus, cellulose (4 wt%) was dissolved in LiOH/urea/water (4.6 : 15 : 80.4, weight ratio), whereas chitosan (4 wt%) was dissolved in LiOH/KOH/urea/water (4.6 : 7 : 8 : 80.4, weight ratio). Both solutions were then mixed under high shear, degassed, cast, and regenerated as 1 mm thick films (Fig. 7). At lower pH the swelling of the composite films increased with increasing chitosan content because of higher osmotic pressure, leading to chitosan leaching. Pure cellulose films showed the highest density and best stress-strain properties; both properties decrease with increasing chitosan content. This was attributed to the disruption of the fine structure of cellulose parallel lamellae, leading to a less aligned and more loosely packed microstructure in the NC, as evidenced by SEM and X-ray powder diffraction experiments.

Another method describes the preparation of Cel/Ch composites prepared from the IL 1-butyl-3-methylimidazolium acetate and γ-valerolactone as a sustainable cosolvent (Y. Duan, Freyburger, Kunz

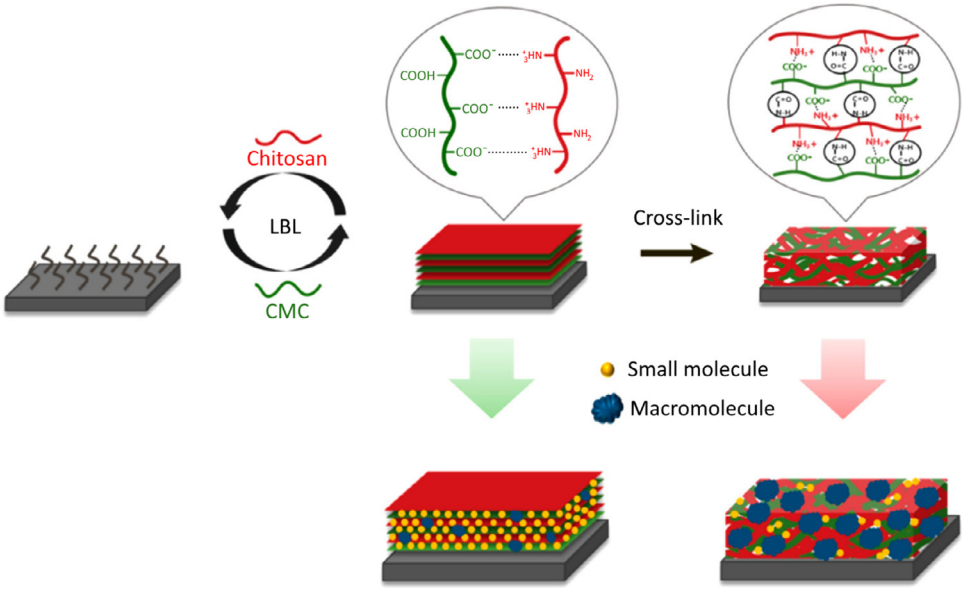

Fig. 6. Schematic illustration of the cross-linking-induced structural change of the CMC/chitosan multilayer film and its effect on the loading of drugs with different molecular weights; adapted with permission from Park et al., (2017), ACS, 2017.

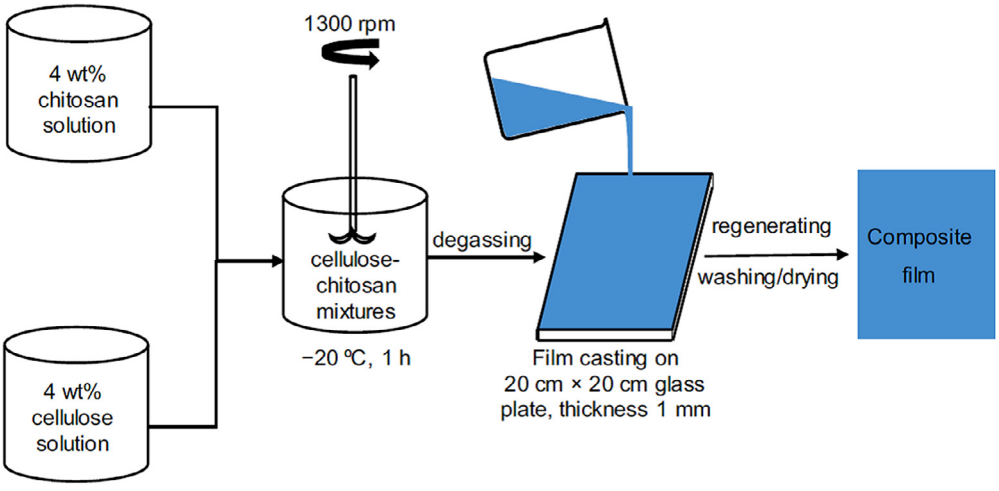

Fig. 7. Scheme of the preparation of Cel/Chs nanocomposite films in aqueous alkaline solutions; reproduced with permission from (J. Yang et al., 2019), Springer, 2019.

& Zollfrank, 2018). First, the biopolymers were dissolved separately in the binary IL/cosolvent solution at 90 °C and then mixed to obtain the desired cellulose/chitin molar ratios. Determination of the mechanical properties of composites revealed that the tensile stress decreases while elastic modulus and elongation at break increases with increasing chitin content. At 20 wt% cellulose and 80 wt% chitin, the composite film had a higher tensile strength (4.7 MPa) than pure the cellulose film (3.3 MPa), which demonstrates the interaction between both polysaccharides, where cellulose is mainly reinforcing the composite material. This can be corroborated by the fact that chitosan, hydroxypropylmethyl cellulose composite films also exhibited better mechanical properties compared to pure chitosan or chitosan/pectin composites (Tejada et al., 2017).

Derivatization of the polysaccharides may affect the mechanical properties as shown when oxidized cellulose sulfate (by sodium periodate) and commercial carboxymethyl chitosan (degree of carboxymethylation = 1) composites were fabricated. Each component was dissolved in a phosphate-buffer (polymer concentration = 0.09 mmol/ml) and then different mixing ratios of oxidized cellulose sulfate and carboxymethyl chitosan were prepared (1:1 to 1:10 by volume). The two biopolymer derivatives were covalently crosslinked *via* reductive amination. It was found that the storage modulus G' is dependent on the molar masses of the polymers and the crosslink density, i.e., on the amount of available aldehyde groups of the oxidized cellulose sulfate because it determines the number of possible cross-links (Strätz & Fischer, 2020).

Due to the inherent biocompatibility of these biopolymers, their use in biomedical applications is self-evident. Additionally, derivatization of cellulose, chitin and chitosan may improve solubility and biological interactions. Thus, chitosan/hydroxypropylmethyl cellulose films were prepared by solution blending and characterized in terms of morphology, mechanical properties, adhesiveness, swelling, and drug release (Tejada et al., 2017). The 0.2–0.7 mm thick films were loaded with miconazole nitrate (used to treat fungal skin infections, *candidiasis*) and efficient in vitro antifungal activity was found. For fluconazole buccal delivery (drug used to treat serious fungal or yeast infections), thiolated bucco-adhesive films based on chitosan and CMC were developed (Naz et al., 2017). Because weak film adhesion is often the bottleneck for buccal-therapeutic applications, both polysaccharides were chemically modified. Thus, chitosan was modified with thioglycolic acid, and CMC with L-Cysteine. Both derivatives were then dissolved in water, the solutions were mixed at different (volume) ratios, and glycerol (plasticizer) and fluconazole added. After drying at 60 °C a thin flexible film was formed. A comparison with the unmodified polysaccharide compos-

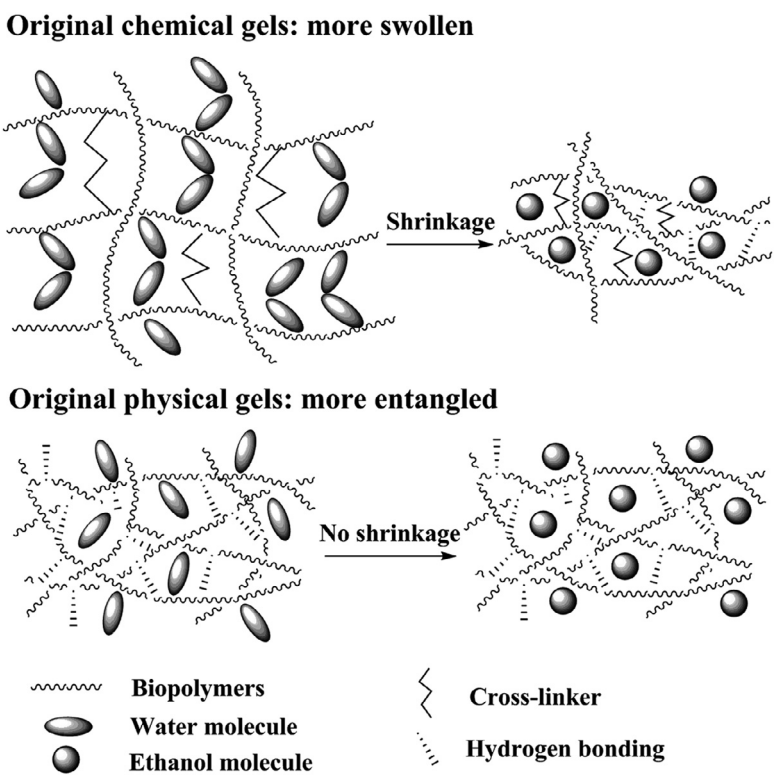

Fig. 8. Proposed shrinkage mechanism of chemical and physical gels caused by solvent exchange and supercritical CO_2 ($ScCO_2$)-drying: polymer chains of chemical crosslinked hydrogels are likely to be less intertwined than those in physical gels due to the presence of the crosslinker, when immersed in ethanol and then $ScCO_2$-dried, the stretched biopolymer chains in chemical hydrogels can be re-entangled resulting in significant shrinking; reprinted with permission from (Shen et al., 2016), ACS, 2016.

ite films revealed 2-fold higher water binding capacity, 6-fold higher muco-adhesiveness, and 17-fold higher drug transport. The latter was attributed to the interaction of cysteine-rich subdomains of mucus glycoproteins with the polysaccharide SH groups *via* thiol/disulfide exchange reactions (Figure SI-8).

An interesting strategy to achieve antibacterial properties is the functional finishing of textiles. For instance, water soluble *O*-acrylamidomethyl-*N*-[(2-hydroxy-3- dimethyldodecyl-ammonium)propyl] chitosan chloride was synthesized by reacting chitosan with epoxypropyldodecyldimethyl quaternary ammonium salt and *N*-methylolacrylamide. The derivative forms covalent bonds with the textile fabric. The treated cotton fabrics showed durable antimicrobial functions even after 30 consecutive launderings, and improved uptakes, fixation rates, and fastness of reactive dyes without using an auxiliary electrolyte (Pan et al., 2020). More information about Cel/Ch/Chs based antibacterial materials (Khattak et al., 2019) and antimicrobial textile treatments (Shahid-ul-Islam & Butola, 2019) can be found in recent reviews.

3.3. Miscellaneous shapes

We address here Cel/Ch/Chs composite materials different in shape from those discussed above. This includes, e.g., hydrogels, scaffolds and spheres. Hydrogels are three-dimensional hydrophilic polymeric networks with the ability to absorb large amounts of liquids. They can be obtained by physical or chemical crosslinking. Physical hydrogels are based on polymer chain entanglements, van der Waals forces, H-bonds, hydrophobic or coulombic interactions. Chemical hydrogels are prepared with the help of a cross-linking agent to form covalent bonds between the component polymers. For cellulose, chitin and chitosan the cross-linking is established, e.g., by esterification with dicarboxylic acids. When the gels are freed from solvents (water or alcohols), they remain as porous polymer scaffolds (Shen et al., 2016).

Hydrogels prepared from chitin and cellulose extracted with 1-ethyl-3-methylimidazolium acetate from dried/processed shrimp shells (Shamshina et al., 2014) and wood biomass, respectively, were compared with hydrogels prepared from commercially available chitin and MCC; aerogels were fabricated as well (Shen et al., 2016). Low molar mass pure chitin was not suitable for the preparation of physical or chemical hydrogels. Furthermore, it was concluded that lower molar mass of both polysaccharides requires a crosslinker to obtain stable hydrogels. Up to 98% shrinking of chemically crosslinked gels was observed, whereas the physical gels hardly suffered from shrinking, especially when supercritical CO_2-drying was employed. A possible mechanistic explanation is given in Fig. 8. Dye loading and release studies on the gels suggested their potential use to effectively load and release active species for pharmaceutical applications.

Porous thermosensitive hydrogel blends from chitosan, CMC and glycerol 2-phosphate exhibited a sol/gel phase transition at 32–35 °C, which was employed to solidify the fluid inside hydatid cysts (a parasitic disease of tapeworms of the *Echinococcus* type) for effective control of spillage during the aspiration of hydatid cysts (Azadi, Hassanjili, Zarrabi & Sarkari, 2018). The hydrogel was prepared by mixing chitosan dissolved in diluted acetic acid with CMC/glycerol 2-phosphate aqueous solutions. The final composite contained 1–2 wt% chitosan, 0.8–1.6 wt% CMC, and 2–5.9 wt% glycerol 2-phosphate. Alamar Blue cytotoxicity assays showed that the composite had no significant cytotoxic effect on human fibroblast cells. Thermosensitive hydrogels were also prepared on the basis of chitosan, hydroxypropylmethyl cellulose and glycerol (T. Wang et al., 2016). Additional literature on cellulose and Cel/Ch based hydrogel materials have been reviewed recently (Kabir et al., 2018; (Shen et al., 2016b)).

There is an increased interest in hydrogels with self-healing properties because their strong tissue adhesion significantly promotes wound healing. They may also transport therapeutic agents to the damaged tissue area, leading to a local treatment effect. Moreover, these hydrogels may provide an extracellular matrix-like 3D environment for embedded cells and thus have potential application in tissue engineering. Thus, chitosan/polyethylene glycol/cellulose nanofiber (CNFs) composites hydrogels were fabricated by suspending CNFs into a chitosan solution in the presence of 4-formylbenzoic acid cross-linking agent. The self-healing property can be controlled by the amounts of CNFs

and the cross-linking agent. Neural stem cells embedded in the chitosan/CNFs hydrogel with the best self-healing properties (CNFs range investigated = 0.06–0.15 wt%, best performance at 0.09 wt% of CNFs) reveal significantly enhanced oxygen metabolism as well as neural differentiation. Moreover, the neural regeneration effect of the optimized chitosan-CNFs shows a 50% improvement over the pristine chitosan hydrogel in the zebrafish brain injury model. The new self-healing hydrogels provide design rationale for hydrogels with better injectability and tissue regeneration potential (Cheng, Huang, Wei & Hsu, 2019).

Self-repairing hydrogels can also be prepared from low degree-substituted ferrocene-cellulose and cyclodextrin-chitosan (Duan et al., 2015). Therefore, both derivatives were dissolved in LiCl/*N,N*-dimethylformamide (DMF) and the mixture was cast into appropriate molds. The self-healing mechanism is explained by intermolecular inclusion complex formation between the ferrocene and cyclodextrin moieties that are covalently bond to the polysaccharide backbones, see Figure SI-9.

Hydroxyethyl chitosan/cellulose scaffolds for bone tissue engineering were prepared by co-dissolving both polysaccharides in LiOH/urea/water and subsequent cross-linking with epichlorohydrin (Y. Wang et al., 2017). Characterization of the properties revealed that the addition of hydroxyethyl chitosan to cellulose improved compressive modulus, wettability and elasticity of the scaffolds. The composite scaffolds also supported osteoblastic MC3T3-E1 cells to attach, grow and proliferate, which is suitable for bone regeneration materials. CMC/chitosan composite sponges may pose as carrier for drugs such as gentamicin, ibuprofen and roxithromycin (B. Cai et al., 2018). The CMC/chitosan ratio and pH significantly affected the microstructure the sponge, its degradation behavior, drug loading capacity and the antibacterial activity (*E. Coli*).

Different types of Cel/Chs NCs in the form of spherical particles of different sizes were prepared. Both polysaccharides were previously dissolved: cellulose in LiOH/urea, and chitosan in LiOH/KOH/urea or acetic acid. The particles were obtained by dripping the cellulose solution into a solution of chitosan in a dilute acetic acid. Cel/Chs microspheres with and without the addition of crosslinking agent were prepared *via* sol-gel transition in water-in-oil emulsions, see Figure SI-10 (J. Yang et al., 2016). Magnetic Cel/Chs microspheres were synthesized by dissolving 7 wt% of the polysaccharides (weight ratio 1:2) in 1-butyl-3-methylimidazolium chloride and adding Fe_3O_4 nanoparticles (Peng et al., 2017). Due to its nanoporous structure and large quantity of carboxyl groups, the Cel/Chs microspheres exhibited excellent adsorption performance for removal of Pb(II) ions and methylene blue from aqueous solutions.

Mucoadhesive microspheres with diameters from 460 to 860 μm were prepared from chitosan and hydroxypropylmethyl- or methylcellulose to control drug delivery (antiulcer drug) and improve its bioavailability (Khattab & Zaki, 2017). The best results with respect to drug entrapment efficiency, swelling index, release time and mucoadhesive properties were obtained with microspheres consisting of high molecular mass chitosan and hydroxypropylmethyl cellulose dissolved in acetic acid. Trivedi et al. describe a simple approach to design cytocompatible, nontoxic, and multifunctional Cel/Chs hydrogel beads by dissolving the polysaccharides in NaOH/urea/water and coagulating them under acidic conditions (Trivedi et al., 2018). The acids used as coagulation medium were acetic-, hydrochloric-, and sulfuric acid. They were evaluated regarding their effect on blend morphology; acetic acid showed the best results. The composites cytocompatibility was assessed on human breast adenocarcinoma cells. Osteoblast growth and adhesion over 8 days could be achieved, which allows future in vitro studies for breast cancer and bone regeneration.

Cu (II) ions were removed from aqueous solutions with Cel/Chs spheres prepared from IL/*N,N*-dimethylformamide solutions (Wittmar, Klug & Ulbricht, 2020). The authors showed that maximum adsorption capacities increase with increasing number of amino groups, i.e., chitosan present in the blend. Adsorption kinetic and thermodynamic studies on Cel/Chs aerogels with Congo red found maximum removal efficiency at a composition ratio of 1:3 by weight (Wang et al., 2018b).

Conclusions

Cellulose, chitin and chitosan are structurally related, renewable, low-cost biopolymers with increasing importance due to the growing need to find sustainable alternatives of synthetic polymers for certain applications. Their functional groups (OH, CH_3CONH-, and -NH_2) interact strongly with each other at the molecular level, leading to formation of relatively homogeneous NCs. These are most conveniently fabricated by biopolymer solution mixing, followed by product regeneration into different physical “shapes”, e.g., fibers, films, and hydrogels. Common solvents that dissolve cellulose, chitin and chitosan include ILs, IL/MSs and inorganic alkali/urea. The composition of the produced NCs, hence their physicochemical and biological properties can be controlled by adjusting the concentrations of the precursor components. Cellulose is usually the reinforcing component to provide the NC with enhanced mechanical properties. On the other hand, the biological activity of chitin and chitosan makes them natural candidates for biomedical applications and food packaging materials. Further property “tuning” can be achieved by cross-linking of the polysaccharides and their derivatization. In this regard, polymer degradation during derivatization reactions, and decreased dissolution due to cross-linking are important issues to be addressed, in order to maintain quality of the NCs. To contribute to the continued efforts towards a sustainable future, the concepts of *green chemistry* should be applied for composite fabrication as well. This includes process optimization, e.g., by using chemometrics, use of environmentally benign solvents and chemicals, recyclability of the solvents employed, and a closer cooperation between researchers in academia and industry.

Author Contributions

The manuscript was written through contributions of the two authors, who approved the final version of the manuscript.

Funding

This work was supported by FAPESP grant numbers 2014/22136-4, 2016/22869-7, and 2017/06394-1.

Acknowledgments

O. A. El Seoud and M. Kostag thank the FAPESP research foundation for financial support, grant numbers 2014/22136-4, 2016/22869-7 and 2017/06394-1. O. A. El Seoud thanks CNPq for research productivity fellowship (grant 306108/2019-4).

Supplementary materials

Supplementary material associated with this article can be found, in the online version, at doi:10.1016/j.carpta.2021.100079.

References

Anderson, J. L., Valderama, D., & Jory, D. E. (2019). *GOAL 2019: Global shrimp production review* November 4. Global Aquaculture Alliance https://www.aquaculturealliance.org/advocate/goal-2019-global-shrimp-production-review/.

Araki, Y., & Ito, E. (1974). A pathway of chitosan formation in Mucor rouxii: Enzymatic deacetylation of chitin. *Biochemical and Biophysical Research Communications, 56*(3), 669–675. https://doi.org/10.1016/0006-291X(74)90657-3.

Azadi, M. D. A., Hassanjili, S., Zarrabi, K., & Sarkari, B. (2018). Solidification of hydatid cyst fluid with an injectable chitosan/carboxymethylcellulose/β-glycerophosphate hydrogel for effective control of spillage during aspiration of hydatid cysts. *Progress in Biomaterials, 7*(1), 35–54. https://doi.org/10.1007/s40204-018-0082-5.

Bassas-Galia, M., Follonier, S., Pusnik, M., & Zinn, M. (2017). Natural polymers: A source of inspiration. In G. Perale, & J. Hilborn (Eds.), *Bioresorbable polymers for biomedical applications* (pp. 31–64). Cambridge, UK: Woodhead Publishing. https://doi.org/10.1016/B978-0-08-100262-9.00002-1.

Blackwell, J. (1988). Physical methods for the determination of chitin structure and conformation. In *Methods in enzymology: 161* (pp. 435–442). Academic Press. https://doi.org/10.1016/0076-6879(88)61053-6.

Boluk, Y. (2005). Acid–base interactions and swelling of cellulose fibers in organic liquids. *Cellulose (London, England), 12*(6), 577–593. https://doi.org/10.1007/s10570-005-9004-5.

Buschle-Diller, G., & Zeronian, S. H. (1992). Enhancing the reactivity and strength of cotton fibers. *Journal of Applied Polymer Science, 45*(6), 967–979. https://doi.org/10.1002/app.1992.070450604.

Cai, B., Zhong, T., Chen, P., Fu, J., Jin, Y., Liu, Y., et al. (2018). Preparation, characterization and in vitro release study of drug-loaded sodium carboxymethylcellulose/chitosan composite sponge. *PloS one, 13*(10), Article e0206275. https://doi.org/10.1371/journal.pone.0206275.

Cai, J., & Zhang, L. (2005). Rapid dissolution of cellulose in LiOH/urea and NaOH/urea aqueous solutions. *Macromolecular Bioscience, 5*(6), 539–548. https://doi.org/10.1002/mabi.200400222.

Catalán, J. (2009). Toward a generalized treatment of the solvent effect based on four empirical scales: Dipolarity (SdP, a new scale), polarizability (SP), acidity (SA), and basicity (SB) of the medium. *The Journal of Physical Chemistry B, 113*(17), 5951–5960. https://doi.org/10.1021/jp8095727.

Catalán, J., & Díaz, C. (1997). A generalized solvent acidity scale: The solvatochromism of o-tert-butylstilbazolium betaine dye and its homomorph o,o′-di-tert-butylstilbazolium betaine dye. *Liebigs Annalen, 1997*(9), 1941–1949. https://doi.org/10.1002/jlac.199719970921.

Chang, K. L. B., Tsai, G., Lee, J., & Fu, W.-. R. (1997). Heterogeneous N-deacetylation of chitin in alkaline solution. *Carbohydrate Research, 303*(3), 327–332. https://doi.org/10.1016/S0008-6215(97)00179-1.

Chen, Y.-. L., Zhang, X., You, T.-. T., & Xu, F. (2019). Deep eutectic solvents (DESs) for cellulose dissolution: A mini-review. *Cellulose (London, England), 26*(1), 205–213. https://doi.org/10.1007/s10570-018-2130-7.

Cheng, K.-. C., Huang, C.-. F., Wei, Y., & Hsu, S. (2019). Novel chitosan—Cellulose nanofiber self-healing hydrogels to correlate self-healing properties of hydrogels with neural regeneration effects. *NPG Asia Materials, 11*(1), 1–17. https://doi.org/10.1038/s41427-019-0124-z.

Deng, Z., Wang, T., Chen, X., & Liu, Y. (2020). Applications of chitosan-based biomaterials: A focus on dependent antimicrobial properties. *Marine Life Science & Technology*. https://doi.org/10.1007/s42995-020-00044-0.

Díez-Pascual, A. M. (2019). Synthesis and applications of biopolymer composites. *International Journal of Molecular Sciences, 20*(9), 2321. https://doi.org/10.3390/ijms20092321.

Driemeier, C., & Calligaris, G. A. (2011). Theoretical and experimental developments for accurate determination of crystallinity of cellulose I materials. *Journal of Applied Crystallography, 44*(1), 184–192. https://doi.org/10.1107/S0021889810043955.

Duan, J., Han, C., Liu, L., Jiang, J., Li, J., Li, Y., et al. (2015). Binding cellulose and chitosan via intermolecular inclusion interaction: Synthesis and characterisation of gel. *Journal of Spectroscopy, 2015*, Article 179258. https://doi.org/10.1155/2015/179258.

Duan, Y., Freyburger, A., Kunz, W., & Zollfrank, C. (2018). Cellulose and chitin composite materials from an ionic liquid and a green co-solvent. *Carbohydrate Polymers, 192*, 159–165. https://doi.org/10.1016/j.carbpol.2018.03.045.

Dumitriu, S. (2004). *Polysaccharides: Structural diversity and functional versatility* (Ed.) (2nd ed.). CRC Press.

Ebnesajjad, S. (2012). *Handbook of biopolymers and biodegradable plastics: Properties, processing and applications* (Ed.). William Andrew. https://doi.org/10.1016/C2011-0-07342-8.

El Seoud, O. A., Bioni, T. A., & Dignani, M. T. (2020a). Understanding cellulose dissolution in ionic liquid-dimethyl sulfoxide binary mixtures: Quantification of the relative importance of hydrogen bonding and hydrophobic interactions. *Journal of Molecular Liquids*, Article 114848. https://doi.org/10.1016/j.molliq.2020.114848.

El Seoud, O. A., Kostag, M., Jedvert, K., & Malek, N. I. (2020b). Cellulose regeneration and chemical recycling: Closing the "cellulose gap" using environmentally benign solvents. *Macromolecular Materials and Engineering*, Article 1900832. https://doi.org/10.1002/mame.201900832.

El-Diasty, E. M., Nesreen, Z. E., & Hoda, A. M. A. (2012). Using of chitosan as antifungal agent in Kariesh cheese. *New York Science Journal, 5*(9), 5–10.

Fidale, L. C., Ruiz, N., Heinze, T., & El Seoud, O. A. (2008). Cellulose swelling by aprotic and protic Solvents: What are the similarities and differences? *Macromolecular Chemistry and Physics, 209*(12), 1240–1254. https://doi.org/10.1002/macp.200800021.

Food and Agriculture Organization of the United Nations. (2019). *GLOBEFISH highlights - Issue 3/2019: A quarterly update on world seafood markets april 2019 issue, with january–december 2018 statistics*. FAO http://www.fao.org/documents/card/en/c/ca5870en/.

Foston, M. (2014). Advances in solid-state NMR of cellulose. *Current Opinion in Biotechnology, 27*, 176–184. https://doi.org/10.1016/j.copbio.2014.02.002.

French, A. D. (2017). Glucose, not cellobiose, is the repeating unit of cellulose and why that is important. *Cellulose (London, England), 24*(11), 4605–4609. https://doi.org/10.1007/s10570-017-1450-3.

Fukuda, H. (1980). Polyelectrolyte complexes of chitosan with sodium carboxymethylcellulose. *Bulletin of the Chemical Society of Japan, 53*(4), 837–840. https://doi.org/10.1246/bcsj.53.837.

Galanakis, C. M. (2015). Separation of functional macromolecules and micromolecules: From ultrafiltration to the border of nanofiltration. *Trends in Food Science & Technology, 42*(1), 44–63. https://doi.org/10.1016/j.tifs.2014.11.005.

Galanakis, C. M. (2020). The food systems in the era of the coronavirus (COVID-19) pandemic crisis. *Foods (Basel, Switzerland), 9*(4), 523. https://doi.org/10.3390/foods9040523.

Galanakis, C. M. (2021). Functionality of food components and emerging technologies. *Foods (Basel, Switzerland), 10*(1), 128. https://doi.org/10.3390/foods10010128.

Gardner, K. H., & Blackwell, J. (1974). The structure of native cellulose. *Biopolymers, 13*(10), 1975–2001. https://doi.org/10.1002/bip.1974.360131005.

Gardner, K. H., & Blackwell, J. (1975). Refinement of the structure of β-chitin. *Biopolymers, 14*(8), 1581–1595. https://doi.org/10.1002/bip.1975.360140804.

Glasser, W. G., Atalla, R. H., Blackwell, J., Brown, R. M., Burchard, W., French, A. D., et al. (2012). About the structure of cellulose: Debating the Lindman hypothesis. *Cellulose (London, England), 19*(3), 589–598. https://doi.org/10.1007/s10570-012-9691-7.

Gooday, G. W. (1990). The ecology of chitin degradation. In K. C. Marshall (Ed.), *Advances in microbial ecology* (pp. 387–430). Springer US. https://doi.org/10.1007/978-1-4684-7612-5_10.

Gooday, G. W., Jeuniaux, C., & Muzzarelli, R. (1986). *Chitin in nature and technology* (Eds.). Springer US. https://doi.org/10.1007/978-1-4613-2167-5.

Haghighi, H., Licciardello, F., Fava, P., Siesler, H. W., & Pulvirenti, A. (2020). Recent advances on chitosan-based films for sustainable food packaging applications. *Food Packaging and Shelf Life, 26*, Article 100551. https://doi.org/10.1016/j.fpsl.2020.100551.

Hamed, I., Özogul, F., & Regenstein, J. M. (2016). Industrial applications of crustacean by-products (chitin, chitosan, and chitooligosaccharides): A review. *Trends in Food Science & Technology, 48*, 40–50. https://doi.org/10.1016/j.tifs.2015.11.007.

Hanabusa, H., Izgorodina, E. I., Suzuki, S., Takeoka, Y., Rikukawa, M., & Yoshizawa-Fujita, M. (2018). Cellulose-dissolving protic ionic liquids as low cost catalysts for direct transesterification reactions of cellulose. *Green Chemistry, 20*(6), 1412–1422. https://doi.org/10.1039/C7GC03603E.

Hasegawa, M., Isogai, A., Onabe, F., & Usuda, M. (1992). Dissolving states of cellulose and chitosan in trifluoroacetic acid. *Journal of Applied Polymer Science, 45*(10), 1857–1863. https://doi.org/10.1002/app.1992.070451020.

Hauru, L. K. J., Hummel, M., King, A. W. T., Kilpeläinen, I., & Sixta, H. (2012). Role of solvent parameters in the regeneration of cellulose from ionic liquid solutions. *Biomacromolecules, 13*(9), 2896–2905. https://doi.org/10.1021/bm300912y.

Hayashi, N., Sugiyama, J., Okano, T., & Ishihara, M. (1997). Selective degradation of the cellulose Iα component in Cladophora cellulose with Trichoderma viride cellulase. *Carbohydrate Research, 305*(1), 109–116. https://doi.org/10.1016/S0008-6215(97)00281-4.

Heinze, T., El Seoud, O. A., & Koschella, A. (2018). Structure and properties of cellulose and its derivatives. In *Cellulose derivatives* (pp. 39–172). Cham, Switzerland: Springer. https://doi.org/10.1007/978-3-319-73168-1_2.

Hu, D., Wang, H., & Wang, L. (2016). Physical properties and antibacterial activity of quaternized chitosan/carboxymethyl cellulose blend films. *LWT - Food Science and Technology, 65*, 398–405. https://doi.org/10.1016/j.lwt.2015.08.033.

Indumathi, M. P., Saral Sarojini, K., & Rajarajeswari, G. R. (2019). Antimicrobial and biodegradable chitosan/cellulose acetate phthalate/ZnO nano composite films with optimal oxygen permeability and hydrophobicity for extending the shelf life of black grape fruits. *International Journal of Biological Macromolecules, 132*, 1112–1120. https://doi.org/10.1016/j.ijbiomac.2019.03.171.

Ishida, T. (2020). Theoretical investigation of dissolution and decomposition mechanisms of a cellulose fiber in ionic liquids. *The Journal of Physical Chemistry B, 124*(15), 3090–3102. https://doi.org/10.1021/acs.jpcb.9b11527.

John, M.J., .& Thomas, S. (2012). Natural polymers: An overview. In *Natural Polymers* (Vol. 1, pp. 1–7). https://doi.org/10.1039/9781849735193-00001.

Johnson, E. L., & Peniston, Q. P. (1982). Utilization of shellfish waste for chitin and chitosan production. In R. E. Martin (Ed.), *Chemistry & biochemistry of marine food products* (p. 415). AVI Publishing Co Inc.

Kabir, S. M. F., Sikdar, P. P., Haque, B., Bhuiyan, M. A. R., Ali, A., & Islam, M. N. (2018). Cellulose-based hydrogel materials: Chemistry, properties and their prospective applications. *Progress in Biomaterials, 7*(3), 153–174. https://doi.org/10.1007/s40204-018-0095-0.

Kestur, G. S. (2010). Biodegradable polymer composites based on Brazilian lignocellulosic. *Matéria, 15*(2), 88–95. https://doi.org/10.1590/S1517-70762010000200001.

Khanafari, A., Marandi, R., & Sanatei, S. (2008). Recovery of chitin and chitosan from shrimp waste by chemical and microbial methods. *Journal of Environmental Health Science & Engineering, 5*(1), 1–24.

Khattab, A., & Zaki, N. (2017). Optimization and evaluation of gastroretentive ranitidine HCl microspheres by using factorial design with improved bioavailability and mucosal integrity in ulcer model. *AAPS PharmSciTech, 18*(4), 957–973. https://doi.org/10.1208/s12249-017-0744-y.

Khattak, S., Wahid, F., Liu, L.-. P., Jia, S.-. R., Chu, L.-. Q., Xie, Y.-. Y., et al. (2019). Applications of cellulose and chitin/chitosan derivatives and composites as antibacterial materials: Current state and perspectives. *Applied Microbiology and Biotechnology, 103*(5), 1989–2006. https://doi.org/10.1007/s00253-018-09602-0.

Klemm, D., Schmauder, H.-. P., & Heinze, T. (2005). Cellulose. *Biopolymers online*. American Cancer Society. https://doi.org/10.1002/3527600035.bpol6010.

Köhler, S., Liebert, T., & Heinze, T. (2009). Ammonium-based cellulose solvents suitable for homogeneous etherification. *Macromolecular Bioscience, 9*(9), 836–841. https://doi.org/10.1002/mabi.200900156.

Kostag, M., & El Seoud, O. A. (2019). Dependence of cellulose dissolution in quaternary ammonium-based ionic liquids/DMSO on the molecular structure of the electrolyte. *Carbohydrate Polymers, 205*, 524–532. https://doi.org/10.1016/j.carbpol.2018.10.055.

Kostag, M., Gericke, M., Heinze, T., & El Seoud, O. A. (2019). Twenty-five years of cellulose chemistry: Innovations in the dissolution of the biopolymer and its transformation into esters and ethers. *Cellulose (London, England), 26*(1), 139–184. https://doi.org/10.1007/s10570-018-2198-0.

Kramer, K. J., Hopkins, T. L., & Schaefer, J. (1995). Applications of solids NMR to the analysis of insect sclerotized structures. *Insect Biochemistry and Molecular Biology, 25*(10), 1067–1080. https://doi.org/10.1016/0965-1748(95)00053-4.

Kramer, K. J., & Koga, D. (1986). Insect chitin: Physical state, synthesis, degradation and metabolic regulation. *Insect Biochemistry, 16*(6), 851–877. https://doi.org/10.1016/0020-1790(86)90059-4.

Kulshreshtha, A. K., & Vasile, C. (2002). *Handbook of polymer blends and composites*. iSmithers Rapra Publishing (Vol. 1).

Kumar, S., Mukherjee, A., & Dutta, J. (2020). Chitosan based nanocomposite films and coatings: Emerging antimicrobial food packaging alternatives. *Trends in Food Science & Technology, 97*, 196–209. https://doi.org/10.1016/j.tifs.2020.01.002.

Kurita, K., Sannan, T., & Iwakura, Y. (1977). Studies on chitin, 4. Evidence for formation of block and random copolymers of N-acetyl-D-glucosamine and D-glucosamine by hetero- and homogeneous hydrolyses. *Die Makromolekulare Chemie, 178*(12), 3197–3202. https://doi.org/10.1002/macp.1977.021781203.

Lan, W., He, L., & Liu, Y. (2018). Preparation and properties of sodium carboxymethyl cellulose/sodium alginate/chitosan composite film. *Coatings, 8*(8), 291. https://doi.org/10.3390/coatings8080291.

Laurienzo, P. (2010). Marine polysaccharides in pharmaceutical applications: An overview. *Marine Drugs, 8*(9), 2435–2465. https://doi.org/10.3390/md8092435.

Lehane, M. J. (1997). Peritrophic matrix structure and function. *Annual Review of Entomology, 42*(1), 525–550. https://doi.org/10.1146/annurev.ento.42.1.525.

Li, Z., Ma, J., Li, R., Yin, X., Dong, W., & Pan, C. (2018). Fabrication of a blood compatible composite membrane from chitosan nanoparticles, ethyl cellulose and bacterial cellulose sulfate. *RSC Advances, 8*(55), 31322–31330. https://doi.org/10.1039/C8RA05536J.

Liu, J., Kim, H., Dhumal, N. R., & Kim, H. J. (2019). Vibrational spectroscopy of imidazolium-based ionic liquids: A combined MD/DFT study. *Journal of Molecular Liquids, 292*, Article 111282. https://doi.org/10.1016/j.molliq.2019.111282.

Lodhi, G., Kim, Y.-. S., Hwang, J.-. W., Kim, S.-. K., Jeon, Y.-. J., Je, J.-. Y., et al. (2014). Chitooligosaccharide and its derivatives: Preparation and biological applications. *BioMed Research International, 2014*, Article 654913. https://doi.org/10.1155/2014/654913.

Ludwick, A. G., & Aglan, H. A. (2020). Renewability of polymer-based thin films for packaging. In S. Hashmi, & I. A. Choudhury (Eds.), *Encyclopedia of renewable and sustainable materials* (pp. 219–230). Elsevier. https://doi.org/10.1016/B978-0-12-803581-8.11294-9.

Luo, X., & Zhang, L. (2013). New solvents and functional materials prepared from cellulose solutions in alkali/urea aqueous system. *Food Research International, 52*(1), 387–400. https://doi.org/10.1016/j.foodres.2010.05.016.

Ma, G., Yang, D., Zhou, Y., Xiao, M., Kennedy, J. F., & Nie, J. (2008). Preparation and characterization of water-soluble N-alkylated chitosan. *Carbohydrate Polymers, 74*(1), 121–126. https://doi.org/10.1016/j.carbpol.2008.01.028.

Ma, Q., Gao, X., Bi, X., Han, Q., Tu, L., Yang, Y., et al. (2020). Dissolution and deacetylation of chitin in ionic liquid tetrabutylammonium hydroxide and its cascade reaction in enzyme treatment for chitin recycling. *Carbohydrate Polymers, 230*, Article 115605. https://doi.org/10.1016/j.carbpol.2019.115605.

Martínez-Campos, E., Civantos, A., Redondo, J. A., Guzmán, R., Pérez-Perrino, M., Gallardo, A., et al. (2017). Cell Adhesion and proliferation on sulfonated and non-modified chitosan films. *AAPS PharmSciTech, 18*(4), 974–982. https://doi.org/10.1208/s12249-016-0619-7.

Martinou, A., Kafetzopoulos, D., & Bouriotis, V. (1993). Isolation of chitin deacetylase from Mucor rouxii by immunoaffinity chromatography. *Journal of Chromatography A, 644*(1), 35–41. https://doi.org/10.1016/0021-9673(93)80117-Q.

Medronho, B., & Lindman, B. (2015). Brief overview on cellulose dissolution/regeneration interactions and mechanisms. *Advances in Colloid and Interface Science, 222*, 502–508. https://doi.org/10.1016/j.cis.2014.05.004.

Mikhailov, G. M., Lebedeva, M. F., Nud'ga, L. A., & Petrova, V. A. (2001). Composite fibers based on chitin and cellulose. *Russian Journal of Applied Chemistry, 74*(9), 1573–1576. https://doi.org/10.1023/A:1013734008473.

Morais, E. S., Lopes, A. M. da C., Freire, M. G., Freire, C. S. R., Coutinho, J. A. P., & Silvestre, A. J. D. (2020). Use of ionic liquids and deep eutectic solvents in polysaccharides dissolution and extraction processes towards sustainable biomass valorization. *Molecules (Basel, Switzerland), 25*(16), 3652. https://doi.org/10.3390/molecules25163652.

Muzzarelli, R. A. A. (2013). *Chitin*. Elsevier.

n.a. (2020). *Principles of suturing wounds and basic skills: Evidence based review*. https://www.doctors.net.uk/_datastore/ecme/mod1226/Suture%20Evidence%20Based%20Review_for%20proofreading_revised.pdf.

Naz, K., Shahnaz, G., Ahmed, N., Qureshi, N. A., Sarwar, H. S., Imran, M., et al. (2017). Formulation and in vitro characterization of thiolated buccoadhesive film of fluconazole. *AAPS PharmSciTech, 18*(4), 1043–1055. https://doi.org/10.1208/s12249-016-0607-y.

No, H. K., & Hur, E. Y. (1998). Control of foam formation by antifoam during demineralization of crustacean shell in preparation of chitin. *Journal of Agricultural and Food Chemistry, 46*(9), 3844–3846. https://doi.org/10.1021/jf9802676.

Ogawa, K., Yui, T., & Okuyama, K. (2004). Three D structures of chitosan. *International Journal of Biological Macromolecules, 34*(1), 1–8. https://doi.org/10.1016/j.ijbiomac.2003.11.002.

Ottenhall, A., Seppänen, T., & Ek, M. (2018). Water-stable cellulose fiber foam with antimicrobial properties for bio based low-density materials. *Cellulose (London, England), 25*(4), 2599–2613. https://doi.org/10.1007/s10570-018-1738-y.

Pan, H., Zhao, T., Xu, L., Shen, Y., Wang, L., & Ding, Y. (2020). Preparation of novel chitosan derivatives and applications in functional finishing of textiles. *International Journal of Biological Macromolecules, 153*, 971–976. https://doi.org/10.1016/j.ijbiomac.2019.10.226.

Park, S., Choi, D., Jeong, H., Heo, J., & Hong, J. (2017). Drug loading and release behavior depending on the induced porosity of chitosan/cellulose multilayer nanofilms. *Molecular Pharmaceutics, 14*(10), 3322–3330. https://doi.org/10.1021/acs.molpharmaceut.7b00371.

Parviainen, A., King, A. W. T., Mutikainen, I., Hummel, M., Selg, C., Hauru, L. K. J., et al. (2013). Predicting cellulose solvating capabilities of acid–base conjugate ionic liquids. *ChemSusChem, 6*(11), 2161–2169. https://doi.org/10.1002/cssc.201300143.

Peng, S., Liu, Y., Xue, Z., Yin, W., Liang, X., Li, M., et al. (2017). Modified nanoporous magnetic cellulose–chitosan microspheres for efficient removal of Pb(II) and methylene blue from aqueous solution. *Cellulose (London, England), 24*(11), 4793–4806. https://doi.org/10.1007/s10570-017-1463-y.

Percot, A., Viton, C., & Domard, A. (2003). Characterization of shrimp shell deproteinization. *Biomacromolecules, 4*(5), 1380–1385. https://doi.org/10.1021/bm034115h.

Pérez, S., & Samain, D. (2010). Structure and engineering of celluloses. In D. Horton (Ed.), *Advances in carbohydrate chemistry and biochemistry* (pp. 25–116). Academic Press. Vol. 64. https://doi.org/10.1016/S0065-2318(10)64003-6.

Peter, M. G. (2005a). Chitin and chitosan from animal sources. *Biopolymers online*. American Cancer Society. https://doi.org/10.1002/3527600035.bpol6015.

Peter, M. G. (2005b). Chitin and chitosan in fungi. *Biopolymers online*. American Cancer Society. https://doi.org/10.1002/3527600035.bpol6005.

Philipp, B., Schleicher, H., & Wagenknecht, W. (1973). The influence of cellulose structure on the swelling of cellulose in organic liquids. *Journal of Polymer Science: Polymer Symposia, 42*(3), 1531–1543. https://doi.org/10.1002/polc.5070420356.

Philippova, O. E., Korchagina, E. V., Volkov, E. V., Smirnov, V. A., Khokhlov, A. R., & Rinaudo, M. (2012). Aggregation of some water-soluble derivatives of chitin in aqueous solutions: Role of the degree of acetylation and effect of hydrogen bond breaker. *Carbohydrate Polymers, 87*(1), 687–694. https://doi.org/10.1016/j.carbpol.2011.08.043.

Pillai, C. K. S., Paul, W., & Sharma, C. P. (2009). Chitin and chitosan polymers: Chemistry, solubility and fiber formation. *Progress in Polymer Science, 34*(7), 641–678. https://doi.org/10.1016/j.progpolymsci.2009.04.001.

Pinkert, A., Marsh, K. N., & Pang, S. (2010). Reflections on the solubility of cellulose. *Industrial & Engineering Chemistry Research, 49*(22), 11121–11130. https://doi.org/10.1021/ie1006596.

Pires, P. A. R., Malek, N. I., Teixeira, T. C., Bioni, T. A., Nawaz, H., & El Seoud, O. A. (2015). Imidazole-catalyzed esterification of cellulose in ionic liquid/molecular solvents: A multi-technique approach to probe effects of the medium. *Industrial Crops and Products, 77*, 180–189. https://doi.org/10.1016/j.indcrop.2015.08.015.

Poletto, M., Ornaghi, H. L., & Zattera, A. J. (2014). Native cellulose: Structure, characterization and thermal properties. *Materials, 7*(9), 6105–6119. https://doi.org/10.3390/ma7096105.

Priyadarshi, R., & Rhim, J.-. W. (2020). Chitosan-based biodegradable functional films for food packaging applications. *Innovative Food Science & Emerging Technologies, 62*, Article 102346. https://doi.org/10.1016/j.ifset.2020.102346.

Reichardt, C., & Welton, T. (2010). Empirical parameters of solvent polarity. In *Solvents and solvent effects in organic chemistry* (pp. 425–508). Weinheim, Germany: Wiley-VCH Verlag GmbH & Co. KGaA. https://doi.org/10.1002/9783527632220.ch7.

Roberts, G. A. F. (1992). Structure of chitin and chitosan. In G. A. F. Roberts (Ed.), *Chitin chemistry* (pp. 1–53). Macmillan Education UK. https://doi.org/10.1007/978-1-349-11545-7_1.

Sannan, T., Kurita, K., & Iwakura, Y. (1976). Studies on chitin, 2. Effect of deacetylation on solubility. *Die Makromolekulare Chemie, 177*(12), 3589–3600. https://doi.org/10.1002/macp.1976.021771210.

Segal, L., Creely, J. J., Martin, A. E., J., & Conrad, C. M. (1959). An empirical method for estimating the degree of crystallinity of native cellulose using the x-ray diffractometer. *Textile Research Journal, 29*(10), 786–794. https://doi.org/10.1177/004051755902901003.

Shahid-ul-Islam, & Butola, B. S. (2019). Recent advances in chitosan polysaccharide and its derivatives in antimicrobial modification of textile materials. *International Journal of Biological Macromolecules, 121*, 905–912. https://doi.org/10.1016/j.ijbiomac.2018.10.102.

Shamshina, J. L. (2019). Chitin in ionic liquids: Historical insights into the polymer's dissolution and isolation. A review. *Green Chemistry, 21*(15), 3974–3993. https://doi.org/10.1039/C9GC01830A.

Shamshina, J. L., Berton, P., & Rogers, R. D. (2019). Advances in functional chitin materials: A review. *ACS Sustainable Chemistry & Engineering, 7*(7), 6444–6457. https://doi.org/10.1021/acssuschemeng.8b06372.

Shamshina, J. L., Gurau, G., Block, L. E., Hansen, L. K., Dingee, C., Walters, A., et al. (2014). Chitin–calcium alginate composite fibers for wound care dressings spun from ionic liquid solution. *Journal of Materials Chemistry B, 2*(25), 3924–3936. https://doi.org/10.1039/C4TB00329B.

Shamshina, J. L., Zavgorodnya, O., Choudhary, H., Frye, B., Newbury, N., & Rogers, R. D. (2018). In search of stronger/cheaper chitin nanofibers through electrospinning of chitin—Cellulose composites using an ionic liquid platform. *ACS Sustainable Chemistry & Engineering, 6*(11), 14713–14722. https://doi.org/10.1021/acssuschemeng.8b03269.

Shen, X., Shamshina, J. L., Berton, P., Bandomir, J., Wang, H., Gurau, G., et al. (2016a). Comparison of hydrogels prepared with ionic-liquid-isolated vs commercial chitin and cellulose. *ACS Sustainable Chemistry & Engineering, 4*(2), 471–480. https://doi.org/10.1021/acssuschemeng.5b01400.

Shen, X., Shamshina, J. L., Berton, P., Gurau, G., & Rogers, R. D. (2016b). Hydrogels based on cellulose and chitin: Fabrication, properties, and applications. *Green Chemistry, 18*(1), 53–75. https://doi.org/10.1039/C5GC02396C.

Shimo, M., Abe, M., & Ohno, H. (2016). Functional comparison of polar ionic liquids and onium hydroxides for chitin dissolution and deacetylation to chitosan. *ACS Sustainable Chemistry & Engineering, 4*(7), 3722–3727. https://doi.org/10.1021/acssuschemeng.6b00368.

Strätz, J., & Fischer, S. (2020). Tailored covalently cross-linked hydrogels based on oxidized cellulose sulfate and carboxymethyl chitosan by targeted adjustment of the storage modulus. *Cellulose (London, England), 27*(13), 7535–7542. https://doi.org/10.1007/s10570-020-03279-3.

Taheri, N., Abdolmaleki, A., & Fashandi, H. (2018). Pyridinium-based ionic liquid/water mixture intended for efficient dissolution of cellulose, chitosan and chitin: The pivotal contribution of water. *Carbohydrate Polymers, 195*, 413–419. https://doi.org/10.1016/j.carbpol.2018.04.123.

Takegawa, A., Murakami, M., Kaneko, Y., & Kadokawa, J. (2010). Preparation of chitin/cellulose composite gels and films with ionic liquids. *Carbohydrate Polymers, 79*(1), 85–90. https://doi.org/10.1016/j.carbpol.2009.07.030.

Tan, W., Zhang, J., Zhao, X., Li, Q., Dong, F., & Guo, Z. (2020). Preparation and physicochemical properties of antioxidant chitosan ascorbate/methylcellulose composite films. *International Journal of Biological Macromolecules, 146*, 53–61. https://doi.org/10.1016/j.ijbiomac.2019.12.044.

Tejada, G., Barrera, M. G., Piccirilli, G. N., Sortino, M., Frattini, A., Salomón, C. J., et al. (2017). Development and evaluation of buccal films based on chitosan for the potential treatment of oral candidiasis. *AAPS PharmSciTech, 18*(4), 936–946. https://doi.org/10.1208/s12249-017-0720-6.

Tenhunen, T.-. M., Lewandowska, A. E., Orelma, H., Johansson, L.-. S., Virtanen, T., Harlin, A., et al. (2018). Understanding the interactions of cellulose fibres and deep eutectic solvent of choline chloride and urea. *Cellulose (London, England), 25*(1), 137–150. https://doi.org/10.1007/s10570-017-1587-0.

Tokura, S., & Tamura, H. (2007). Chitin and Chitosan. In H. Kamerling (Ed.), *Comprehensive glycoscience* (pp. 449–475). Elsevier. https://doi.org/10.1016/B978-044451967-2/00127-6.

Trivedi, P., Saloranta-Simell, T., Maver, U., Gradišnik, L., Prabhakar, N., Smått, J.-. H., et al. (2018). Chitosan—Cellulose multifunctional hydrogel beads: Design, characterization and evaluation of cytocompatibility with breast adenocarcinoma and osteoblast cells. *Bioengineering, 5*(1), 3. https://doi.org/10.3390/bioengineering5010003.

Tsigos, I., Martinou, A., Kafetzopoulos, D., & Bouriotis, V. (2000). Chitin deacetylases: New, versatile tools in biotechnology. *Trends in Biotechnology, 18*(7), 305–312. https://doi.org/10.1016/S0167-7799(00)01462-1.

Uto, T., Idenoue, S., Yamamoto, K., & Kadokawa, J. (2018). Understanding dissolution process of chitin crystal in ionic liquids: Theoretical study. *Physical Chemistry Chemical Physics, 20*(31), 20669–20677. https://doi.org/10.1039/C8CP02749H.

Utracki, L. A. (1999). Polymer blends: Fundamentals. In J. Karger-Kocsis (Ed.), *Polypropylene: An A-Z reference* (pp. 601–605). Netherlands: Springer. https://doi.org/10.1007/978-94-011-4421-6_81.

Valizadeh, S., Naseri, M., Babaei, S., Hosseini, S. M. H., & Imani, A. (2019). Development of bioactive composite films from chitosan and carboxymethyl cellulose using glutaraldehyde, cinnamon essential oil and oleic acid. *International Journal of Biological Macromolecules, 134*, 604–612. https://doi.org/10.1016/j.ijbiomac.2019.05.071.

Vanapalli, K. R., Sharma, H. B., Ranjan, V. P., Samal, B., Bhattacharya, J., Dubey, B. K., et al. (2021). Challenges and strategies for effective plastic waste management during and post COVID-19 pandemic. *Science of The Total Environment, 750*, Article 141514. https://doi.org/10.1016/j.scitotenv.2020.141514.

Vermeulen, C. A., & Wessels, J. G. H. (1986). Chitin biosynthesis by a fungal membrane preparation. *European Journal of Biochemistry, 158*(2), 411–415. https://doi.org/10.1111/j.1432-1033.1986.tb09768.x.

Wang, H., Qian, J., & Ding, F. (2018a). Emerging chitosan-based films for food packaging applications. *Journal of Agricultural and Food Chemistry, 66*(2), 395–413. https://doi.org/10.1021/acs.jafc.7b04528.

Wang, T., Chen, L., Shen, T., & Wu, D. (2016a). Preparation and properties of a novel thermo-sensitive hydrogel based on chitosan/hydroxypropyl methylcellulose/glycerol. *International Journal of Biological Macromolecules, 93*, 775–782. https://doi.org/10.1016/j.ijbiomac.2016.09.038.

Wang, Tuo, Yang, H., Kubicki, J. D., & Hong, M. (2016b). Cellulose structural polymorphism in plant primary cell walls investigated by high-field 2D solid-state NMR spectroscopy and density functional theory calculations. *Biomacromolecules, 17*(6), 2210–2222. https://doi.org/10.1021/acs.biomac.6b00441.

Wang, Y., Qian, J., Zhao, N., Liu, T., Xu, W., & Suo, A. (2017). Novel hydroxyethyl chitosan/cellulose scaffolds with bubble-like porous structure for bone tissue engineering. *Carbohydrate Polymers, 167*, 44–51. https://doi.org/10.1016/j.carbpol.2017.03.030.

Wang, Y., Wang, H., Peng, H., Wang, Z., Wu, J., & Liu, Z. (2018b). Dye adsorption from aqueous solution by cellulose/chitosan composite: Equilibrium, kinetics, and thermodynamics. *Fibers and Polymers, 19*(2), 340–349. https://doi.org/10.1007/s12221-018-7520-9.

Wang, Z., Hu, Q., Dai, X., Wu, H., Wang, Y., & Shen, J. (2009). Preparation and characterization of cellulose fiber/chitosan composites. *Polymer Composites, 30*(10), 1517–1522. https://doi.org/10.1002/pc.20724.

Wittmar, A. S. M., Klug, J., & Ulbricht, M. (2020). Cellulose/chitosan porous spheres prepared from 1-butyl-3-methylimidazolium acetate/dimethylformamide solutions for Cu2+ adsorption. *Carbohydrate Polymers, 237*, Article 116135. https://doi.org/10.1016/j.carbpol.2020.116135.

Xu, A., Zhang, Y., Zhao, Y., & Wang, J. (2013a). Cellulose dissolution at ambient temperature: Role of preferential solvation of cations of ionic liquids by a cosolvent. *Carbohydrate Polymers, 92*(1), 540–544. https://doi.org/10.1016/j.carbpol.2012.09.028.

Xu, F., Yu, J., Tesso, T., Dowell, F., & Wang, D. (2013b). Qualitative and quantitative analysis of lignocellulosic biomass using infrared techniques: A mini-review. *Applied Energy, 104*, 801–809. https://doi.org/10.1016/j.apenergy.2012.12.019.

Yang, J., Dahlström, C., Edlund, H., Lindman, B., & Norgren, M. (2019). PH-responsive cellulose–chitosan nanocomposite films with slow release of chitosan. *Cellulose (London, England), 26*(6), 3763–3776. https://doi.org/10.1007/s10570-019-02357-5.

Yang, J., Duan, J., Zhang, L., Lindman, B., Edlund, H., & Norgren, M. (2016). Spherical nanocomposite particles prepared from mixed cellulose–chitosan solutions. *Cellulose (London, England), 23*(5), 3105–3115. https://doi.org/10.1007/s10570-016-1029-4.

Yang, J., Kwon, G., Hwang, K., & Kim, D. (2018). Cellulose—Chitosan antibacterial composite films prepared from LiBr solution. *Polymers, 10*(10), 1058. https://doi.org/10.3390/polym10101058.

Younes, I., & Rinaudo, M. (2015). Chitin and chitosan preparation from marine sources. Structure, properties and applications. *Marine Drugs, 13*(3), 1133–1174. https://doi.org/10.3390/md13031133.

Youssef, Ahmed. M., EL-Sayed, S. M., EL-Sayed, H. S., Salama, H. H., & Dufresne, A. (2016). Enhancement of Egyptian soft white cheese shelf life using a novel chitosan/carboxymethyl cellulose/zinc oxide bionanocomposite film. *Carbohydrate Polymers, 151*, 9–19. https://doi.org/10.1016/j.carbpol.2016.05.023.

ZabihiSahebi, A., Koushkbaghi, S., Pishnamazi, M., Askari, A., Khosravi, R., & Irani, M. (2019). Synthesis of cellulose acetate/chitosan/SWCNT/Fe_3O_4/TiO_2 composite nanofibers for the removal of Cr(VI), As(V), Methylene blue and Congo red from aqueous solutions. *International Journal of Biological Macromolecules, 140*, 1296–1304. https://doi.org/10.1016/j.ijbiomac.2019.08.214.

Zavgorodnya, O., Shamshina, J. L., Bonner, J. R., & Rogers, R. D. (2017). Electrospinning biopolymers from ionic liquids requires control of different solution properties than volatile organic solvents. *ACS Sustainable Chemistry & Engineering, 5*(6), 5512–5519. https://doi.org/10.1021/acssuschemeng.7b00863.

Zhou, J., & Zhang, L. (2000). Solubility of cellulose in NaOH/urea aqueous solution. *Polymer Journal, 32*(10), 866–870. https://doi.org/10.1295/polymj.32.866.

Zhu, K., Wang, Y., Lu, A., Fu, Q., Hu, J., & Zhang, L. (2019). Cellulose/chitosan composite multifilament fibers with two-switch shape memory performance. *ACS Sustainable Chemistry & Engineering, 7*(7), 6981–6990. https://doi.org/10.1021/acssuschemeng.8b06691.